Front. Phys., 2013, 8(6): 794–827
DOI 10.1007/s11467-013-0330-z

REVIEW ARTICLE

Status of dark matter detection

Xiao-Jun Bi†, **Peng-Fei Yin**, **Qiang Yuan**

Key Laboratory of Particle Astrophysics, Institute of High Energy Physics, Chinese Academy of Sciences, Beijing 100049, China
E-mail: †*bixj@ihep.ac.cn*

Received January 23, 2013; accepted April 2, 2013

The detection of dark matter has made great progresses in recent years. We give a brief review on the status and progress in dark matter detection, including the progresses in direct detection, collider detection at LHC and focus on the indirect detection. The results from PAMELA, ATIC, Fermi-LAT and relevant studies on these results are introduced. Then we give the progress on indirect detection of gamma rays from Fermi-LAT and ground based Cerenkov telescopes. Finally the detection of neutrinos and constraints on the nature of dark matter are reviewed briefly.

Keywords dark matter, annihilation, cosmic rays, gamma rays

PACS numbers 12.60.Jv, 14.80.Ly

Contents

1 Introduction

1.1 Astronomical evidence

The standard cosmology is established in the last decade, thanks to the precise cosmological measurements, such as the cosmic microwave background (CMB) radiation measured by WMAP [1, 2], the distance-redshift relation of the Type Ia supernovae [3–5] and the large scale structure (LSS) survey from SDSS [6, 7] and 6df [8]. The energy budget in the standard cosmology consists of 4% baryonic matter, 23% dark matter (DM) and 73% dark energy (DE) [9, 10]. To unveil the mystery of the dark

Frontiers of Physics

side of the Universe is a fundamental problem of modern cosmology and physics. In this review we focus on the progress in DM detection.

Actually the existence of DM has been established for a much longer time. The most direct way that indicates the existence of DM is from the rotation curve of spiral galaxies [11]. The rotation curve shows the rotation velocity of an object around the galaxy center as a function of radius r, which scales like $\sqrt{M(r)/r}$ with $M(r)$ the mass within the orbit r. The rotation curve should decrease as $1/\sqrt{r}$ if r is beyond most of the visible part of the galaxy. However, most measured rotation curves keep flat at large distances. The large rotation velocity implies a dark halo around the galaxy to provide larger centripetal force that exerts on the object.

At the scale of galaxy clusters, evidence of DM is also ample. The first evidence of DM was from the observation of the Coma cluster by Zwicky in 1930s [12]. He found unexpected large velocity dispersion of the member galaxies, which implied the existence of "missing mass" to hold the galaxies [12]. The observation of X-ray emission of hot gas in the clusters can give precise measurement of the gravitational potential felt by the gas to keep the hot gas in hydrostatic equilibrium. Other measurement of weak lensing effect on the background galaxies by the clusters gives direct indication of DM component in clusters. Especially the bullet cluster gives strong support to the DM component in cluster. The Bullet cluster consists of two colliding galaxy clusters. The X-ray image, which reflects the gas component of the colliding system, shows obvious lag compared with the gravitational lensing image, which traces the mass distribution [13]. It is easy to understand that the gas is decelerated due to the viscosity, while the DM component can pass through each other without collision. The Bullet cluster was regarded as the most direct evidence of DM.

The existence of DM in the cosmological scale is inferred by a global fit to the CMB, supernovae and LSS data. The WMAP data give the most accurate determination of the DM component in the universe with $\Omega_{\rm CDM}h^2 = 0.112 \pm 0.006$ [9], with h the Hubble constant in unit of 100 km·s^{-1}·Mpc^{-1}.

1.2 Detection methods

All the current evidence of DM comes from the gravitational effect by DM. From the point of view that all the matter in the universe comes from a big-bang a sole DM component with only gravitational interaction is hard to properly account for the observed DM. A popular DM candidate is the weakly interacting massive particle (WIMP). In such scenario the WIMPs can reach thermal equilibrium in the early universe and decouple from the thermal equilibrium when the temperature decreases. The relic density of WIMPs can be calculated by solving the Boltzmann equation. A good approximate solution of the Boltzmann equation gives

$$\Omega_{\rm DM}h^2 \sim \frac{3\times10^{-27}{\rm cm}^3\cdot{\rm s}^{-1}}{\langle\sigma v\rangle} \quad (1)$$

where $\Omega_{\rm DM} = \rho_{\rm DM}/\rho_0$ is the DM density over the critical density, h is the Hubble constant, $\langle\sigma v\rangle$ is the thermal averaged DM annihilation cross section times velocity. We often refer $\langle\sigma v\rangle$ as the DM annihilation cross section. It represents the interaction strength of the DM particles and the standard model (SM) particles. $\langle\sigma v\rangle = 3\times10^{-26}{\rm cm}^3\cdot{\rm s}^{-1}$ gives the correct relic density and is often taken as the benchmark value for the DM annihilation cross section. It is found a WIMP with mass and interaction strength at the weak scale can easily give correct relic density. If such a scenario is confirmed, it will become the third evidence supporting the hot big bang cosmology after CMB and the big bang nucleosynthesis. Probing such a decoupling process enables us to study the universe as early as its temperature was ~GeV. It has become a fundamental problem to detect the DM particles and determine its nature in cosmology and particle physics. WIMPs, interacting weakly with the SM particles, make it possible to detect the DM in experiments. A great deal of WIMP candidates have been proposed, such as the lightest neutralino in the supersymmetric (SUSY) model and the lightest Kaluza-Klein particle in the Universal extra dimension model (for a review see Ref. [14]).

Figure 1 shows the scheme to probe the DM particles. To determine the nature of DM particles we have

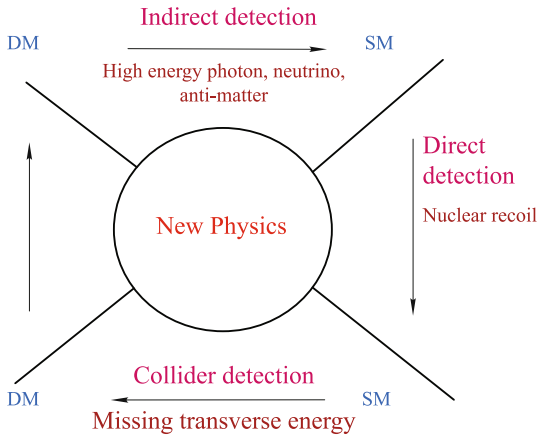

Fig. 1 Schematic plot to show the relation among the *direct detection*, *indirect detection* and *collider detection* of DM. The arrows indicate the direction of reaction.

to study the interaction between the DM and the SM particles. In general there are three different directions to study the interaction. One direction is to search for the scattering signal between DM particle and the detector nucleon. It is called the *direct detection* of DM. The *indirect detection* is to detect the annihilation or decay products of DM particles. Finally the *collider detection* is to search for the DM production process in high energy particle collisions. The three ways of DM detection are not independent, but complementary to each other.

In this review we will focus on the latest progresses of the *indirect detection* of DM. The status of direct detection and collider detection is briefly summarized.

2 Status of direct detection

2.1 Recoil event rate

Direct detection searches for the nuclear recoil signals which are induced by the scattering of DM particles against the target nuclei in the underground detectors [15] (for reviews, see Refs. [16–20]). For the DM with mass of $\sim O(10^2)$ GeV and local velocity of $\sim 10^{-3}c$, the typical energy scale of the recoil signal is $O(10)$ keV. The expected differential event rate per nucleus is

$$\frac{\mathrm{d}R}{\mathrm{d}E_R} = \frac{\rho_\chi}{m_\chi}\int_{v_{min}}^{v_{max}} \mathrm{d}^3v\ f(\vec{v})v\frac{\mathrm{d}\sigma(\vec{v},E_R)}{\mathrm{d}E_R} \qquad (2)$$

where E_R is the nuclear recoil energy, ρ_χ is the local DM mass density, $f(\vec{v})$ is the velocity distribution of DM in the lab frame, $\mathrm{d}\sigma/\mathrm{d}E_R$ is the cross section of the scattering between the DM and target nucleus. Different experiment material and techniques are sensitive to search for different interactions between the DM and nucleus.

In the non-relativistic limit, the interaction between DM and the nuclei can be divided into two classes: the spin-independent (SI) and spin-dependent (SD). The SI interaction couples to the mass of the detector nuclei while the SD couples to the spin of the nuclei. Coherent SI interaction between DM and the nuclei leads to an enhancement of the scattering rate $\sigma \propto A^2$.

2.2 Experimental results

The key issue for direct detection is to control the background (for detailed discussions on backgrounds at the direct detections, see Ref. [19]). To shield the huge background from cosmic rays the detectors are usually located in deep underground laboratory. Since the gamma photons and electrons from the radioactive isotopes in the surrounding rock, air and the detector apparatus will induce electronic recoils in the detector, good shielding and high purity of material for detector are required. Note that the characteristics of electronic recoil events are different from nuclear recoil signals. Many techniques have been developed to distinguish them. Moreover the electron recoil events are often produced in the surface of the detector. Therefore the outer part of detector volume can be used to veto background.

Recently, more than 20 direct detection experiments worldwide are running or under construction. Three kinds of signals namely scintillation, ionization, and photon can be used to record the recoil events. Some experiments detect one kind of signal, while some experiments can measure a combination of two kinds of signals to discriminate the electronic and nuclear recoils. According to the detection technique and the detector material, these experiments fall into different classes, such as scintillator experiments (e.g. DAMA [21], KIMS [22]), cryogenic crystal experiments (e.g. CDMS [23], CoGeNT [24], CRESST [25], EDELWEISS [26], TEXONO [27], CDEX [28]), noble liquid experiments (e.g. XENON [29], ZEPLIN [30], PandaX [31]), superheated liquid experiments (e.g. COUPP [32], PICASSO [33], SIMPLE [34]), etc.

Up to now, most of the direct detection experiments do not observe any DM induced nuclear recoil events and set stringent constraints on the DM-nucleon scattering cross section. However, the following experiments claim they have observed some signal-like events.

- DAMA is a NaI scintillator detector located in Gran Sasso. DAMA collaboration reported an annual modulation effect with a high confidence level $\sim 8.2\sigma$ in the 2–6 keVee energy interval [21, 35]. Such result is consistent with expectation of DM events. Due to the Earth rotation around the Sun, the variation of DM flux will lead to a $\sim 7\%$ anual modulation of the scattering event rate. If DAMA result is induced by DM-nucleus elastic SI scattering, a kind of DM particle with mass of ~ 10 GeV and scatting cross section of $\sim O(10^{-40})$ cm^{-2} is needed [36, 37]. Such light DM can be provided in many theoretical framework, such as SUSY [38–40], asymmetric DM [41], mirror DM [42], etc.
- CoGeNT is a cryogenic germanium detector with a low energy threshold. CoGeNT collaboration reported an excess of events with energy smaller than 3 keVee in 2010 [24] and an annual modulation signal with 2.8σ confidence level in 2011 [43]. Such results can be explained by a DM with mass of ~ 10 GeV and scatting cross section of 10^{-41}–10^{-40}cm^{-2} [44, 45] (see also Refs. [46–48]) which is roughly con-

sistent with that needed for DAMA [49, 50].

- CRESST-II is a Calcium Tungstate ($CaWO_4$) detector which measures both scintillation and phonon signals. In 2011, CRESST-II collaboration reported an excess of events in the 10–40 keV energy interval [25] which is consistent with a 10–30 GeV DM interpretation [51].

The results of DAMA, CoGeNT and CRESST-II seem inconsistent with the results by other experiments with higher sensitivity, such as XENON [29, 52] and CDMS [53], which give null results. Therefore, the nature of these anomalous events are still unclear. There are discussions about the possibility that the DAMA events are induced by atmospheric muon or radioactive isotopes in the literature [54, 55]. If DAMA, CoGeNT and CRESST-II results are produced by ordinary SI DM, it means there exist large experimental uncertainties in the other experiments [49], which seems unacceptable. The astrophysical uncertainties arising from DM velocity distribution are not sufficient to relax such tensions either [56, 57]. Many exotic DM models have been proposed, such as isospin violation DM [45, 58, 59], momentum dependent scattering DM [60, 61], inelastic DM [62, 63] or a combination of them [64]. These models are becoming difficult to explain all the experiment results simultaneously with improvement of CDMS and XENON sensitivity [29].[1)] For instance, inelastic DM model is strongly constrained by the new XENON100 results [29, 68].

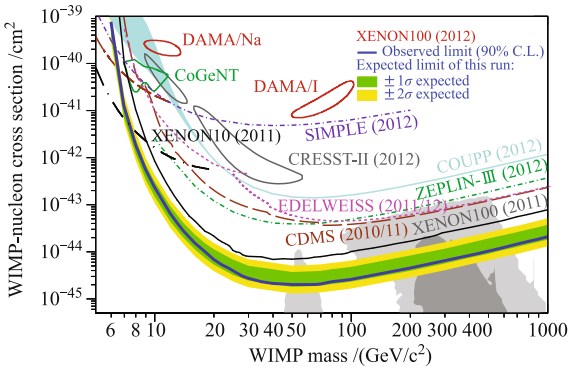

Fig. 2 Constraints on SI DM-nucleon scattering cross section by XENON100. For comparison, other results from DAMA [21, 36], CoGeNT [24], CRESST-II [25], CDMS [23, 53], EDELWEISS [26], SIMPLE [34], COUPP [32], ZEPLIN-III [30] and XENON10 [52], are also shown, together with the preferred regions in CMSSM [69–71]. Reproduced from Ref. [29].

XENON experiment is a dual phase noble liquid detector located in Gran Sasso with simultaneous measurements of the primary scintillation (S1) and secondary ionization signals (S2). The ratio of the two kinds of signals can be used to discriminate the electronic and nuclear recoil events. The most stringent constraints on SI DM-nucleon cross section are set by XENON100 with the exposure of 34×224.6 kg days [29] (for the constraints on SD cross section, see Section 6.2). For DM with mass of 55 GeV, the upper-limit reaches 2×10^{-45} cm^2. It has excluded some preferred parameter regions of the CMSSM. Especially, the pure higgsino DM is strongly disfavor due to large expected SI cross section.

Recently many experiment collaborations are preparing for upgrading their detectors to larger volume. The sensitivities for SI DM-nucleon scattering cross section will be improved by a magnitude of two orders in the next five years [72].

3 Status of collider detection

Since the DM mass is usually assumed to be $\lesssim O(10^2)$ GeV, the DM particles are expected to be generated at the high energy colliders, such as Tevatron [73], LHC [74, 75] and ILC [76]. Once produced, these particles escape the detector without energy deposit due to their extremely weak interactions. Such signal, named "missing transverse energy" (MET), can be reconstructed by the associated jets, photons, or leptons based on momentum conservation in the plane perpendicular to the beam pipe.[2)] It is possible to determine the DM mass at the colliders (see Refs. [77–80] and references therein). Moreover, searches for DM particles and MET signals are essential to determine the mass spectra and typical parameters of the new physics models (for some reviews, see Refs. [81, 82]). It will reveal the origin of electroweak symmetry breaking and the nature of new fundamental symmetries.

At the hadron colliders, the main SM backgrounds arise from the processes which produce neutrinos, such as $Z(\to \nu\bar{\nu})$+jets, $W(\to l\nu)$+jets, $t\bar{t}$ and single top production. Another background is the "fake MET". It arises from the QCD multi-jets due to the fact that the reconstruction of jet has uncertainties. Since the MET induced by DM is related to DM mass, large MET cut condition, e.g. $\not{E}_{\rm T} > 100$ GeV, is often adopted to reduce background.

Frontiers of Physics

[1)] For the constraints from indirect detections on the isospin violation DM, see Refs. [65–67].

[2)] In fact, the variable reconstructed directly is the "missing transverse momentum" $\vec{\not{p}}_{\rm T}$. MET $\not{E}_{\rm T}$ is the magnitude of $\vec{\not{p}}_{\rm T}$. Since the exact energies of initial partons are unknown, only MET is meaningful at the hadron colliders. It is possible to reconstruct the total missing energy at the e^+e^- colliders.

3.1 Direct production

Direct production means the DM particles are produced in pair by the collisions of high-energy SM particles. Since the DM particle pair can not be observed, an additional energetic jet or photon from initial state radiation is needed to trigger the event and to reconstruct MET. Such signal is called "mono-jet" or "mono-photon".[3)] Searching for Mono-jet is more important at the hadron colliders due to large event rate [85–88], while the Mono-photon signal is essential at the e^+e^- colliders [89–91].

To constrain the nature of DM by searching the collider monojet events is usually finished in a model-independent way. The effective field theory is used to describe the interaction between the DM and SM particles [85, 86, 92–95]. For each interaction form, the constraints on the DM mass and interaction coupling can be derived by the results from collider detection, direct detection, indirect detection and DM relic density.

Figure 3 shows the ATLAS limits on SI, SD DM-nucleon scattering and DM annihilation cross sections [74]. Four typical DM-quark interaction operators and one DM-gluon interaction operator [86] are considered in the ATLAS mono-jet analysis. From Fig. 3 we can see the DM searches at the LHC have some advantages compared with the other detections.

- Since the light DM has large production cross section due to the phase space and parton distribution function, LHC has good sensitivity for DM with a mass below 10 GeV. While the sensitivities of direct detection decrease quickly in this region due to the detector energy threshold.
- Since the scalar and axial-vector operators have similar behaviors in the relativistic limit at the colliders, the LHC constraints on SI and SD DM-nucleon scattering can be comparable. For DM with a mass of $O(10)$ GeV, the LHC limits on SI scattering $\sim O(10^{-39})$ cm^2 are weaker than XENON limits. However, the LHC limits on SD scattering $\sim O(10^{-40})$ cm^2 are much better than the results from direct detections.
- If DM interaction with gluon is significant, the production cross section of $gg \to \chi\bar{\chi}$ will be very large at the LHC due to parton distribution function. Therefore LHC has strong capability to detect such DM. The LHC constraints on SI DM-nucleon scattering induced by DM-gluon interaction can be comparable with XENON limits.

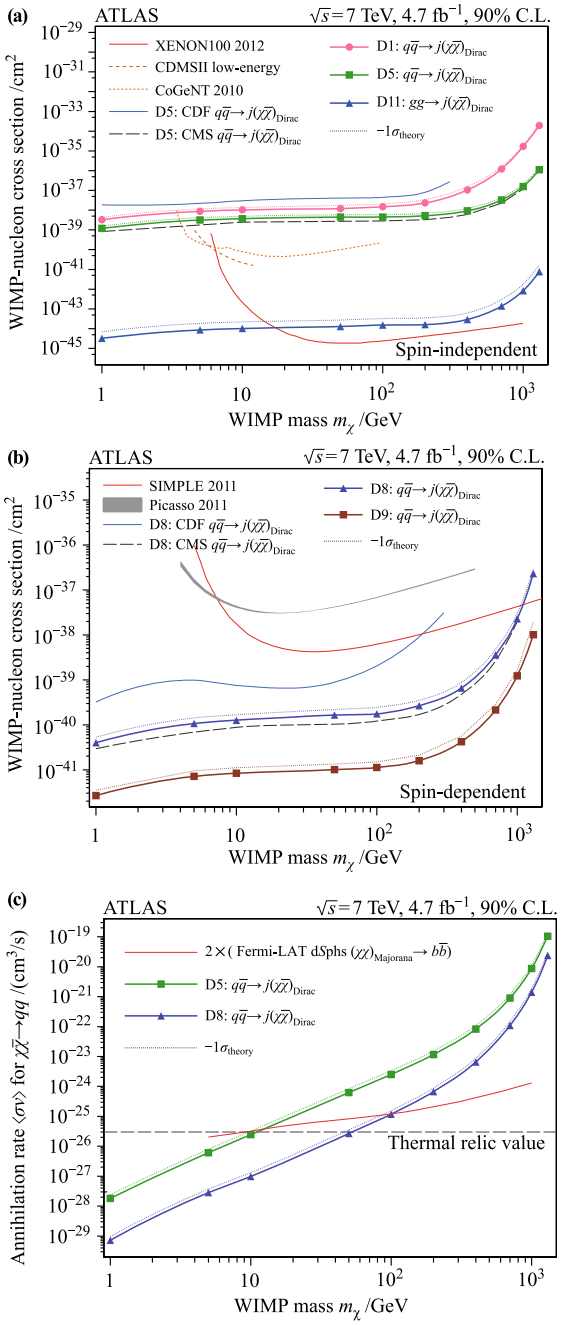

Fig. 3 Inferred ATLAS 90% limits on SI (*top*) and SD (*middle*) DM-nucleon scattering cross section, and ATLAS 95% limits on DM annihilation cross section (*bottom*). D1, D5, D8, D9 and D11 denote the effective interaction operators $\chi\bar{\chi}q\bar{q}$ (scalar), $\chi\gamma^\mu\bar{\chi}q\gamma_\mu\bar{q}$ (vector), $\chi\gamma^\mu\gamma^5\bar{\chi}q\gamma_\mu\gamma_5\bar{q}$ (axial-vector), $\chi\sigma^{\mu\nu}\bar{\chi}q\sigma_{\mu\nu}\bar{q}$ (tensor) and $\chi\bar{\chi}(G^a_{\mu\nu})^2$ (scalar) respectively [86]. For comparison, the limits from XENON100 [29], CDMS [53], CoGeNT [24], SIMPLE [34], PICASSO [33], CDF [73], CMS [96] and Fermi-LAT [97] are also shown. Reproduced from Ref. [74].

[3)] In principle, charged lepton from W [83] or Z boson [84] coming from initial state radiation can also be used to trigger the event, it is called "mono-lepton" or "mono-Z".

It should be noticed that the constraints derived in effective theory is only valid under some assumptions. The effective theory requires the particle that mediates the interaction between DM and SM particles be very heavy, and can be integrated out at the collider energy scale. If the s-channel mediator is light, the event rate will fall with jet transverse energy as $1/p_t^2$, while the event rate is flat with jet p_t in the effective theory. In this case the limits are not applicable [86, 90, 98].

3.2 Indirect production

Indirect production means the DM particles are produced by the cascade decays of some heavier new particles. The most important example is the supersymmetry (SUSY) model.[4)] The LHC can produce pairs of squarks and gluinos via strong interaction processes $pp \to \tilde{q}\tilde{q}$, $\tilde{g}\tilde{g}$ and $\tilde{q}\tilde{g}$, with large cross section. If R-parity is conserved, such particles will decay into the lighter sparticles until the decay chain ends up in the lightest supersymmetry particle (LSP). The final states depend on the mass spectra and decay mode of the sparticles. The typical SUSY signal is usually classified according to jet, b-jet and lepton multiplicity [99, 100], such as jets+MET, 1 b-jet+jets+MET, 1 lepton+jets+MET, two opposite sign leptons+jets+MET (OS), two same sign leptons+jets+MET (SS), etc.

If the dominated decay channels of squarks and gluino are $\tilde{q} \to q\chi$ and $\tilde{g} \to qq'\chi$, the typical signals are 2–4 jets+MET. If the squarks and gluino are much heavier than neutralino, the leading jets are energetic and the reconstructed MET is large. By choosing suitable cut conditions, the SM backgrounds can be suppressed efficiently [101, 102]. A number of kinetic variables, such as effective mass [102], razo [103, 104], α_T [105, 106] and M_{T2} [107–109], are also helpful to discriminate signals and background. Since no excess above SM predictions has been confirmed, the ATLAS and CMS collaborations have set stringent constraints on the masses of gluino and the first two generations of squarks. Figure 4 shows the upper-limits in the CMSSM framework in the m_0-$m_{1/2}$ plane for $\tan\beta = 10$ and $A_0 = 0$ based on CMS results with $\sqrt{s} = 7$ TeV and 4.7 fb^{-1} of data [101]. For all gluino(squarks) masses, squarks(gluino) with masses below ~1200 GeV (800 GeV) have been excluded.

The mass constraints on stop and sbottom are much weaker. It is well-known that the lighter stop can be the lightest colored sparticle due to the larger top Yukawa coupling and large mass splitting terms in many SUSY models. The light stop is also well-motivated by the "naturalness" argument [112, 113], and is consistent with recent LHC Higgs results [114, 115]. Light stop/sbottom can be produced by the decays of gluinos $\tilde{g} \to t\tilde{t}/b\tilde{b}$ which are not very heavy as suggest in the "natural SUSY" framework [113]. It is called gluino-mediated stop/sbottom production. The final states may contain many b-jets due to the processes of $\tilde{t} \to t\chi \to bW^+\chi$, $\tilde{t} \to b\tilde{\chi}^+$ and $\tilde{b} \to b\chi$ which are helpful to reduce backgrounds. For the gluinos with masses below 1 TeV, the DM masses are excluded up to ~500 GeV (300 GeV) for $\tilde{g} \to t\bar{t}\chi(\tilde{g} \to b\bar{b}\chi)$ channel by the recent LHC results [75, 106, 109, 116, 117].

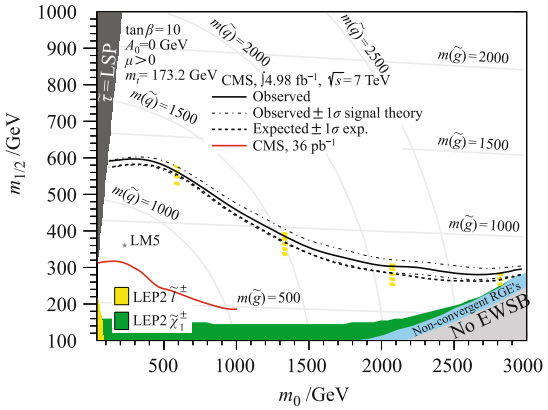

Fig. 4 The CMS limits in the CMSSM $m_0 - m_{1/2}$ plane. The other CMSSM parameters are $\tan\beta = 10$, $\mu > 0$ and $A_0 = 0$. The limits from CMS search with 36 pb^{-1} [110] of data and LEP [111] are also shown. Reproduced from Ref. [101].

If gluino is very heavy, the main production process of stop/sbottom is directly pair production $pp \to t\tilde{t}/b\tilde{b}$. For light stop, the constraints depend on the mass splitting between stop and neutralino, and the assumptions of stop decay modes [113, 118, 119]. The constraints for decay mode $\tilde{t} \to t\chi$ are very stringent in the $m_\chi - m_{\tilde{t}}$ plane [120, 121]. If stop and neutralino are almost degenerate in mass as suggested by the "stop co-annihilation" scenario, the dominated stop decay mode may be flavor changing neutral current $\tilde{t} \to c\chi$. In this case, since the charm jet from stop decay may be too soft, an additional energetic jet is required to reconstruct the MET [122] (see also Refs. [123, 124] and references therein). The constraints for such signal channel are weak.

In many SUSY frameworks, sparticles in the electroweak sector namely neutralinos, charginos and sleptons, are much lighter than colored sparticles. These sparticles can be pair produced via Drell–Yan processes at the colliders [125, 126]. For the neutralino–chargino pair production $pp \to \tilde{\chi}^+\tilde{\chi}_2^0$, the final states may include three charged leptons produced by $\tilde{\chi}^+ \to \bar{l}\nu\chi$ and $\tilde{\chi}_2^0 \to l\bar{l}\chi$.

[4)] The latest ATLAS and CMS SUSY search results can be found in https://twiki.cern.ch/twiki/bin/view/AtlasPublic/SupersymmetryPublicResults and https://twiki.cern.ch/twiki/bin/view/CMSPublic/PhysicsResultsSUS.

The SM backgrounds can be suppressed sufficiently due to the leptons with opposite sign. For the assumptions of $m_{\tilde{\chi}}^{+} = m_{\tilde{\chi}_2^0}$ and $m_{\tilde{l}} = 0.5(m_{\chi} + m_{\tilde{\chi}^+})$, the DM masses can be excluded up to 250 GeV for chargino masses below 450 GeV by the CMS results [125].

If heavier sparticle is long-lived, it is so-called meta-stable massive particle and can be directly observed by detectors. For instance, if the mass splitting between stop (gluino) and neutralino is extremely small, stop (gluino) will form a bound state namely R-hadron in the hadronization process before its decay (see Refs. [127, 128] and references therein). R-hadron will lose energy in the detector due to strong interaction. Another important example is long-lived stau in the GMSB scenario where the LSP and DM candidate is gravitino [129]. If stau is the NLSP,[5)] it may have a long lifetime due to very weak interaction with gravitino, and can be observed in the inner tracker and outer muon detector. The LHC results can exclude stop masses up to 700 GeV, and stau mass up to 300 GeV if they are meta-stable particles [132, 133].

4 Status of indirect detection–charged particles

4.1 Introduction

The indirect detection searches for the DM annihilation or decay products, including γ-rays, neutrinos and charged anti-particles such as positrons and antiprotons. Since the interstellar space is filled with magnetic fields the charged particles are deflected when propagating in the interstellar space. The source information will get lost and therefore we can only resolve the possible signals of DM in the energy spectra of charged particles. On the contrary the γ-rays and neutrinos can trace back to the sources. We can search for such signals at the directions where the DM density is expected to be high.

There are two kinds of γ-ray spectra can be generated from DM annihilation or decay. The DM particles can annihilate/decay into two photons directly. The photon energy equals approximately to the mass (or half mass for decaying DM) of the DM particle since the DM moves non-relativistically today. Such spectrum is monoenergetic, and is usually thought to be the smoking gun of DM signal, since there is no astrophysical process that can produce such kind of spectrum. But such a process is in general highly suppressed and hard to be detected because the DM particles are neutral and can not couple with photons directly. The process can occur through a loop Feynman diagram that DM first annihilate into two virtual charged particles and then the the virtual charged particles annihilate into two real photons. The DM particles can also annihilate into quarks, gauge bosons and so on, which induce continuous γ-ray spectrum by cascade decays. The continuous γ-rays have much larger flux and easier to be detected. However, it does not have distinctive features from the astrophysical background γ-rays.

Right now there are many cosmic ray (CR) experiments dedicated to look for the DM annihilation signals. To avoid the shield of the atmosphere the instruments are better to be placed in space. The satellite based detector PAMELA and the international space station (ISS) detector AMS02 are the two most important experiments for charged particle detection. Both detectors are magnetic spectrometers that have magnetic field to identify the charge of the incident particles. PAMELA was launched in 2006 and many important results have been published. We will give detailed discussion on the PAMELA results in the following. AMS02 was launched in 2011 and the data taking and analysis are on-going. The first physical result of AMS02 will be released soon in this year. It is expected AMS02 will improve the PAMELA results essentially as it has much larger aperture than PAMELA.

The most sensitive γ-ray detector in space is the satellite based Fermi, which can detect γ-rays from 20 MeV to $\sim$ 300 GeV. The detailed summary of the Fermi results on DM detection will be presented in the next section. The ground based image atmospheric Cerenkov telescopes (IACT) detect very high energy (VHE) γ-rays with energy greater than $\sim$ 100 GeV. With the rapid development of the IACT technology the VHE γ-ray astronomy develops quickly in recent years. We will also describe the status of DM searches with IACTs breifly in the next section.

4.2 Experimental status

The most interesting result on DM indirect detection in the recent years comes from PAMELA, which observed obvious positron excess in the cosmic rays (CRs) [134]. The upper panel of Fig. 5 shows the positron fraction $\phi(e^+)/(\phi(e^-) + \phi(e^+))$ measured by PAMELA and several previous experiments. The black curve shows the expectation of the positron fraction from the conventional CR propagation model. In the conventional model there are no primary positrons, and the positrons are secondary products through the interactions of CRs and

[5)] If neutralino is the NLSP, the typical signals are photons+MET where photon is produced by the decay of neutralino $\chi \to \gamma\tilde{G}$ [130, 131].

the interstellar medium (ISM) during the propagation. Here the expected positron fraction is calculated with the GALPROP package [135]. The propagation parameters used are listed in Table 1. The conventional propagation model can reproduce most of the observed CR data on the Earth. For the calculated curves, a solar modulation under the force field approximation [136] is applied with modulation potential 500 MV. Since below $\sim$ 10 GeV the flux is affected by the solar modulation effect, we will pay more attention on the high energy end. It can seen that above $\sim$ 10 GeV the positron ratio shows an obvious excess beyond the expected background from CR physics.

Table 1 Conventional GALPROP model parameters.

z_h	D_0	δ	ρ_0	v_A	γ_{e^-} [a)]	$\gamma_{\rm nuc}$ [b)]
kpc	$10^{28}\,{\rm cm}^2\cdot{\rm s}^{-1}$		GV	${\rm km}\cdot{\rm s}^{-1}$	γ_1/γ_2	γ_1/γ_2
4	5.5	0.34	4	32	1.60/2.62	1.91/2.39

a) Below/above break rigidity 4 GV.
b) Below/above break rigidity 11 GV.

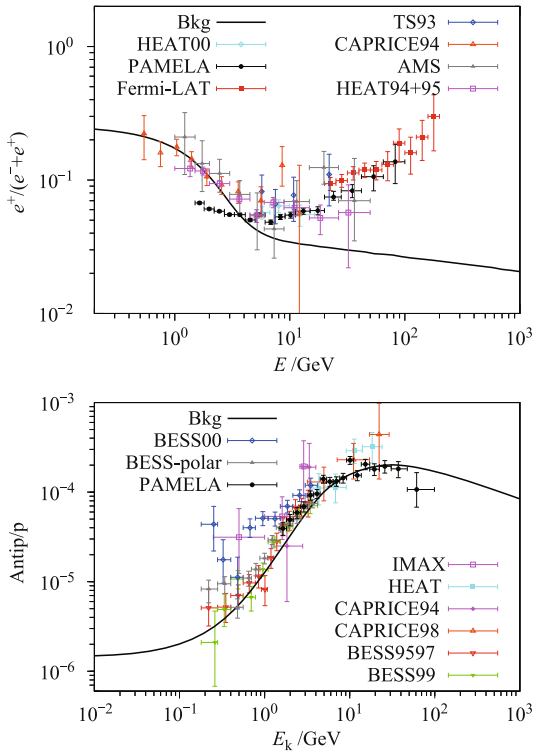

Fig. 5 Observational data of the positron fraction $\phi(e^+)/(\phi(e^-)+\phi(e^+))$ (*upper*) and antiproton-proton ratio $\phi(\bar{p})/\phi(p)$ (*lower*) respectively. Lines in these figures are the expectations based on conventional CR propagation models. The data in the figure are from: positron fraction — TS93 [139], CAPRICE94 [140], AMS [138], HEAT [137, 141], PAMELA [134] and Fermi-LAT [142]; antiproton-proton ratio — IMAX [143], HEAT [144], CAPRICE94 [145], CAPRICE98 [146], BESS95+97 [147], BESS99 [148], BESS00 [148], BESS-polar [149] and PAMELA [150].

In fact, the early HEAT [137] and AMS [138] data have shown the hints of positron excess. The PAMELA data confirmed this excess with high significance [134]. The rise of the positron fraction for energies higher than $\sim$ 10 GeV means that the positron spectrum is even harder than the electron spectrum and cannot be understood easily in the CR background model.

At the same time PAMELA also reported the antiproton-to-proton ratio in CRs [150]. The lower panel of Fig. 5 shows the antiproton-to-proton ratio observed by PAMELA as well as earlier experiments. It shows that the data are well consistent with the expectation of the conventional CR propagation model. The old BESS data are also consistent with background.

Soon after PAMELA released the positron fraction result the balloon-based experiment ATIC published the total electron plus positron spectrum up to about TeV [155]. The ATIC data show a peak between 300 and 800 GeV, together with a sharp falling above 800 GeV [155]. Later Fermi-LAT also measured the total electron spectrum with much larger statistics. Fermi-LAT data give a smooth spectrum with power-law $\sim E^{-3}$ in 20–1000 GeV, without the peak structure as ATIC measured [158]. The ground-based Cerenkov telescope HESS also measured the electron spectrum, which is similar to that from Fermi for $E \lesssim 1$ TeV [157]. Above $\sim$ 1 TeV HESS found a softening of the electron spectrum which is consistent with ATIC data [156]. The observational results are compiled in Fig. 6. The line in Fig. 6 is the expected background contribution of the electrons, which is determined according to the low energy data.

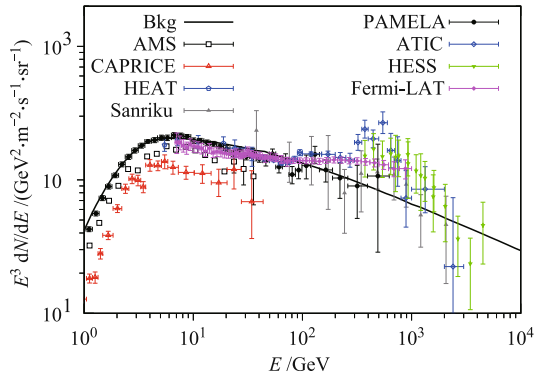

Fig. 6 The electron spectrum. Line in the figure is the expectation based on the conventional CR propagation model. Note that the low energy part of the data are pure electrons, while the high energy data are the sum of electrons and positrons. The data in the figure are from AMS [151], CAPRICE [140], HEAT [152], Sanriku [153], PAMELA [154], ATIC [155], HESS [156, 157] and Fermi-LAT [158].

It should be remarked here that the ATIC and Fermi data of electron spectrum are not consistent with each

other. The ATIC data show sharp feature at ~ 600 GeV, while the Fermi data show a smooth spectrum consistent with a power law. This is the present largest uncertainty to discuss the origin of the positron excess.

One may expect that the hard spectrum as shown for example by the Fermi data could be accounted for by assuming a harder injection spectrum of the background electrons. However, the positron excess in this case will become more significant [159]. Therefore we can conclude that in general it is difficult to reproduce the observed data of both the positron fraction and the electron spectrum under the traditional CR background frame. The data indicate it is most probably that there exists new source(s) of primary electrons and positrons near the solar system.

Those results have stimulated a huge enthusiasm to study the possible origins of the positron and electron excesses. In general all the works can be divided into two classes: the astrophysical origin, such as the nearby pulsar(s) which emit positron/electrons; the exotic origin including DM annihilation or decay. In the following we will give a brief description of the relevant studies.

4.3 Explanations

In the conventional propagation model of Galactic CRs, the source population is often assumed to be one single type and its distribution is usually adopted to be continuous and smooth. The positrons are produced through CR nuclei interacting with the ISM when propagating in the Milky Way. As shown above such a scenario fails to explain the observed positron fraction and electron spectra. To account for the observational data, modifications of the conventional scenario of production and/or propagation of CR electrons and positrons are necessary, through either changing the background model or invoking new sources of $e^{\pm}$. The sources of $e^{\pm}$ generally include: i) secondary production of hadronic cosmic rays interacting with ISM, ii) pair production of photon-photon or photon-magnetic field interactions, iii) pair production of photon-nuclei interactions, and iv) DM annihilation or decay [160]. The two categories of models, astrophysical and DM scenarios, are described in the following in detail respectively.

4.3.1 Astrophysics origins

The first point needs to be clarified is that whether such observational results indeed are "excesses". This depends on the understanding of the background contributions to both the positrons and electrons. The minimal opinion is that there might be no "excess" at all. It was found that there were very large uncertainties of the theoretical expectation of CR positron flux from the primary fluxes of protons and Helium, propagation and hadronic interaction [161]. Therefore it should be more careful to claim an "excess" and judge the amplitude of the "excess" given such large uncertainties. However, it will be difficult to explain the rising behavior of the positron fraction with only the uncertainties, given the fact that the total $e^+ + e^-$ spectrum is as hard as $\sim E^{-3}$ [162, 163]. Through the likelihood analysis with scanning over wide ranges of possible uncertain parameters, significant tension between the $e^{\pm}$ related data and CR nuclei data was found, which implied the "excess" of the $e^{\pm}$ [164].

A less minimal opinion is that the continuous distribution of the CR sources might break down, especially for high energy $e^{\pm}$ which have limited propagation range [165]. The inhomogeneity of supernova remnants (SNRs) leads to distinct features of the primary electron spectrum and may give a rising behavior of the positron fraction. However, the fit to the total electron spectra is poor [165]. Furthermore the result of the positron fraction keeps rising up to 200 GeV, and the positron spectrum is harder than E^{-3} as revealed by Fermi-LAT [142] also disfavor such a scenario with modification of the primary electron spectrum only. Finally it was pointed out that the assumptions of the source distribution in Ref. [165] were too extreme [166].

An alternative scenario without resorting to exotic sources of $e^{\pm}$ is proposed in Ref. [167], where Klein-Nishina suppression of the electron cooling was employed to produce a relatively flat electron spectrum as measured by Fermi-LAT. The PAMELA positron fraction, however, can not be explained with the average parameters of the ISM. To overcome this issue, extremely large values of the starlight intensity and gas density were needed [167].

In summary we can conclude that the current data may still favor the existence of a population of "primary" positrons. There were many astrophysical factories being proposed to produce the high energy electrons/positrons, of which the pulsars are most widely discussed (e.g., [159, 168–173]. The idea of pulsars as the accelerators of high energy electrons/positrons is actually quite old [174–177]. The high energy γ-ray emission of pulsars, especially the recently discovered very high energy emission above 100 GeV [178, 179] directly supports the particle acceleration of pulsars. The strong magnetic field enables the photon-pair cascade occur, makes pulsars natural candidate of positron factory. There are indeed some very nearby pulsars, such as Geminga at 0.16 kpc, PSR B0656+14 at 0.29 kpc and Vela pulsar at 0.29 kpc. Fig. 7 shows an example that a Geminga-like pul-

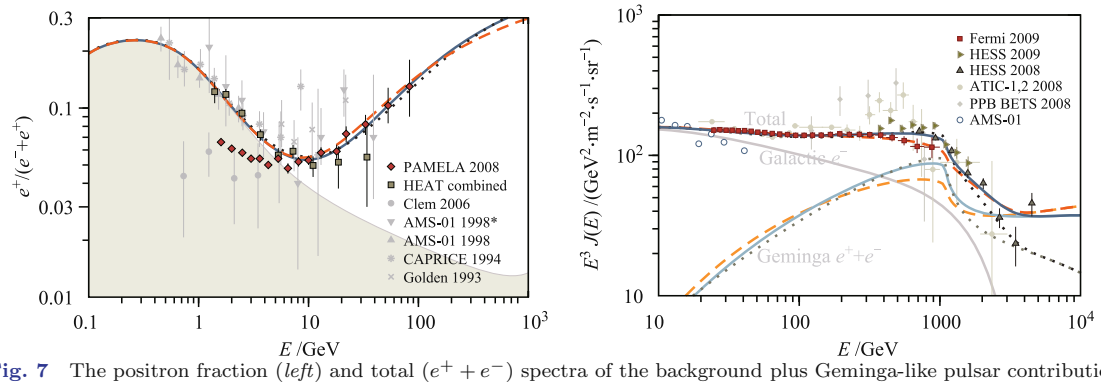

Fig. 7 The positron fraction (*left*) and total ($e^+ + e^-$) spectra of the background plus Geminga-like pulsar contribution. Reproduced from [168].

sar together with the background can explain both the positron fraction and total electron spectra [168]. To fit the data is easy, but to identify which pulsars contribute to the CR leptons is very difficult due to the diffusive propagation of the charged particles. It was discussed that the anisotropy and precise energy spectra of the electrons/positrons might help to identify the sources [169–171, 180].

Other astrophysical sources of the high energy $e^{\pm}$ include secondary $e^{\pm}$ production inside the SNRs [181–183], photo-nuclei pair production of very young SNRs [184], supernova explosion of massive stars [185], γ-ray burst [186], white dwarf "pulsars" [187], pulsar wind nebula [188] and so on. For the scenario of secondary $e^{\pm}$ production inside the SNRs, the expected secondary-to-primary ratio such as $\bar{p}/p$ [189] and B/C [190] will show distinct rising behavior at high energies, and can be tested in future with high precision data.

4.3.2 Dark matter

What is more exciting is that the PAMELA result might be the long-waited DM signal. A lot of works discussed the possibilites that the positron excess comes from DM annihilation or decay. If the positron/electron excesses are due to DM annihilation or decay it gives clear indication of the nature of DM particles. Firstly, since only positron/electron excesses are observed while the antiproton-to-proton ratio is consistent with the CR background prediction, the DM should couple dominantly with leptons. Secondly, the large amount of positrons requires very large annihilation/decay rate of DM. For annihilating DM scenario it requires some non-trivial enhancement mechanisms to get large annihilation cross section. We discuss the first property in the following and leave the discussion of the second point in the next subsection.

Soon after PAMELA reported the new result about the positron fraction, the DM was proposed as a possible positron source to explain the data (e.g., [192, 193]). In [191] we give a careful study of the DM scenario to explain the positron excess. We first assume DM decay[6] into gauge bosons, and the positrons/electrons are then generated from decay of the gauge bosons. Figure 8

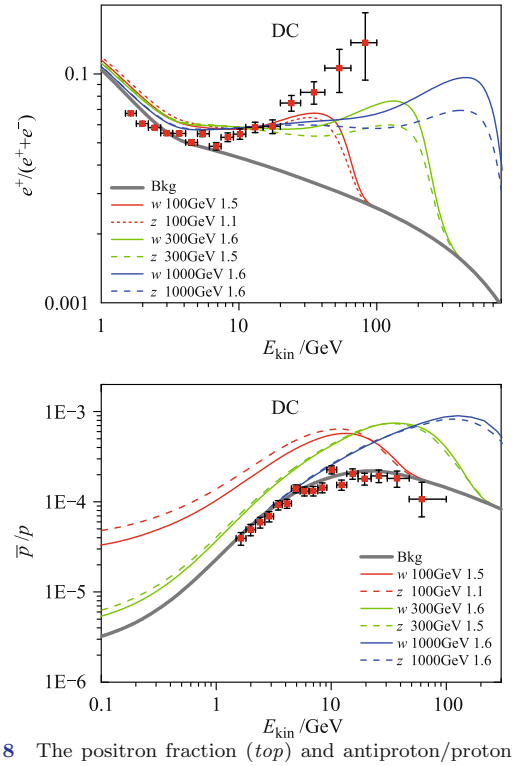

Fig. 8 The positron fraction (*top*) and antiproton/proton ratio (*bottom*) from DM decaying into gauge boson pairs. The grey lines are the background expectation from the CR propagation model. The numbers label the energies of the gauge bosons and the lifetimes of the DM. Reproduced from Ref. [191].

[6] The propagated positron spectra at the Earth from the annihilation scenario and the decay scenario have little difference. Only in the region like the Galactic center the two scenarios show difference. We will discuss the difference in Section 4.5.

shows the calculated positron fraction and antiproton-to-proton ratio for different energies of the gauge bosons. It is shown that the positron spectrum from gauge boson decay is too soft to explain PAMELA data, even the gauge boson mass is as high as 1 TeV. Especially, the gauge boson channel is problematic for the antiproton spectrum. They give several times larger antiproton-to-proton ratio than the PAMELA data. Therefore DM decaying or annihilating to gauge bosons are strongly disfavored by the antiproton data. Similarly we show the case for DM decay into quarks in Fig. 9. Positrons are produced after hadronization of quarks via the decay of charged pions. The positrons are too soft and can not account for the excess of positrons above ~ 10 GeV. Furthermore, quark hadronization produces too many antiprotons, which are several times larger than the PAMELA data. Figure 10 shows the case for lepton channel. It shows that in such case it is easy to account for the PAMELA data by assuming a proper DM mass and life time. Therefore we can conclude that the only possible channel to explain the observed positron excess is DM decay or annihilate into leptons. Similar conclusions were aslo shown in Refs. [194, 195].

Therefore the first important implication for the DM scenario to explain the PAMELA data is that DM has to couple dominantly with leptons.

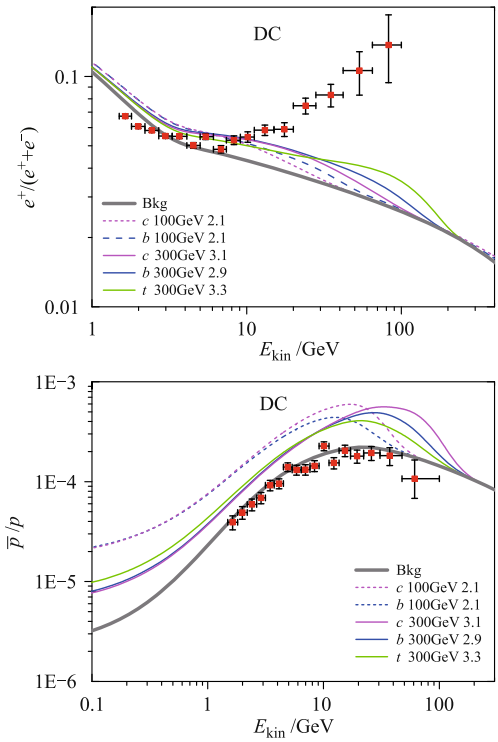

Fig. 9 Same as Fig. 8 but for DM decaying into quark pairs. Reproduced from Ref. [191].

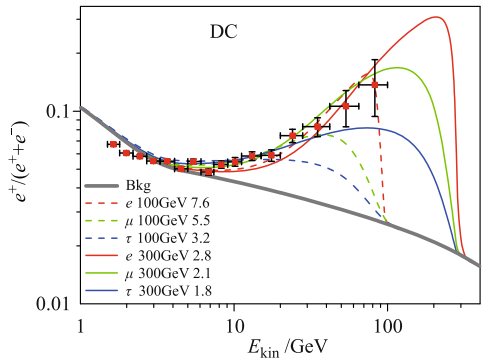

Fig. 10 Positron fraction for DM decaying into lepton pairs. Reproduced from Ref. [191].

4.4 Mechanisms to enhance DM annihilation rate

Another important issue of the DM model to explain the electron/positron excesses is the high production rate of electrons/positrons. For DM annihilation scneario, it means a very large boost factor (BF), the ratio between the required cross section and the benchmark value $3 \times 10^{-26}\mathrm{cm}^3 \cdot \mathrm{s}^{-1}$, at the order $\sim 10^3$ [192, 194]. That is to say to explain the positron excess the DM annihilation rate needs to be about thousand times larger than that to give correct relic density of DM.

There are plenty of papers in the literature to study possible ways to enhance the annihilation rate. The key point here is how to reconcile the large annihilation rate with the much smaller rate at the early time when DM decoupling. We summarize the possible ways in the following.

4.4.1 Substructures

Since the DM annihilation rate is proportional to the density square, the DM substructures are expected to enhance the annihilation rate and give a BF. There have been a lot of careful study on the effect of substructures on charged CRs, based on the N-body simulation results. However, the studies show that the enhancement effects due to substructures is generally negligible [196]. The largest BF with the most extreme configurations of DM substructures is $O(10)$, which is much lower than that needed to explain the PAMELA electron/positron excesses. Considering that the DM velocity in the substructures is smaller than that in the smooth halos, the BF including the Sommerfeld effect is also calculated in [197]. Even in this case the BF is still very small.

It is also proposed that a nearby massive substructure might be able to provide enough BF to explain the data [198]. However, the search in the simulation results shows a very low probability ($\sim 10^{-5}$) of the existence

of such a clump [199]. Therefore it is very difficult to provide a large enough BF to account for the PAMELA electron/positron excesses through DM substructures.

4.4.2 Non-thermal DM

The benchmark value of DM annihilation cross section $3\times10^{-26}\mathrm{cm}^3\cdot\mathrm{s}^{-1}$ is acquired under the assumption that DM is generated thermally in the early universe. If DM is produced by some non-thermal mechanisms, its annihilation cross section is not constrained and can be larger or smaller than the benchmark value.

The non-thermal mechanism is first proposed in Refs. [200, 201], in which DM is generated by the decays of topological defects, such as cosmic string. As PAMELA released the new result the non-thermal mechanism is adopted to explain positron excess. By choosing suitable parameters, the correct relic density and positron flux can be explained simultaneously [202].

It is interesting to note that the non-thermal WIMP from cosmic string decay is more energetic than ordinary WIMP in the early universe, and can be treated as a kind of warm DM. Therefore the free streaming length of non-thermal WIMP may be large. It will lead to distinct predictions of DM substructure and indirect searches from cold WIMP [203].

4.4.3 Breit–Wigner enhancement

If two DM particles annihilate into SM particles through an s-channel process, there is a resonance if the intermediate particle mass is close to $2m_\chi$. This is called the Breit-Wigner enhancement. It is well-known that resonance effect can enhance the DM annihilation cross section significantly [204, 205]. In the Breit–Wigner enhancement scenario [206–209], the DM annihilation process is assumed to be $\chi\bar{\chi}\to R\to f\bar{f}$, where R is a narrow Breit–Wigner resonance with mass $M=\sqrt{4m^2(1-\delta)}$ and decay width $\Gamma=M\gamma$ with $|\delta|,\gamma\ll1$. The annihilation cross section is proportional to

$$\sigma v\propto\frac{1}{(\delta+v^2)^2+\gamma^2} \tag{3}$$

where v is the velocity of two DM particles. From Eq. (3), it can be found that DM particles with smaller v in the halo have larger annihilation cross section than those with larger v in the early universe.

Therefore the Breit–Wigner effect may play a role of BF to explain the PAMELA data [207, 208]. However, to give a large BF required by the electron/positron data at $O(10^3)$, fine tuning of the parameters δ,γ as small as $O(10^{-5})$ is needed [207–209].

Later another important effect, the kinetic decoupling, is discussed [210]. Since after kinetic decoupling the DM particles can not get any momentum exchange with the thermal bath, its velocity decreases more rapidly. As v decreases its annihilation rate is enhanced due to the Breit-Wigner effect and further reduce the relic density of DM significantly. This finally reduce the BF, as shown in Fig. 11. The largest enhancement factor S is at $O(10^2)$ for the DM with a mass of 1 TeV, as shown in Fig. 11. Therefore it is difficult to explain the anomalous positron excesses and give the correct DM relic density simultaneously in the minimal Breit–Wigner enhancement model.

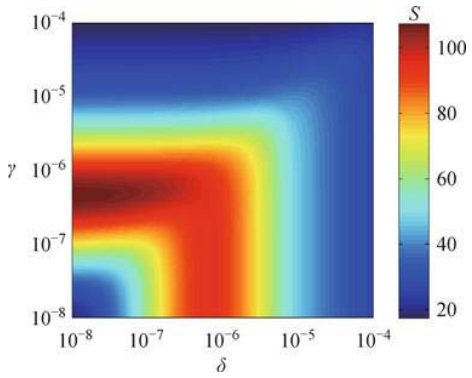

Fig. 11 Numerical illustration of the BF S on the γ–δ parameter plane. Reproduced from Ref. [210].

4.4.4 Sommerfeld enhancement

If there is a long range attractive force between two DM particles, the cross section will enhance at low momentum, known as the Sommerfeld effect. A new light boson ϕ with $m_\phi\ll m_\chi$ is usually assumed to mediate the "long range" interaction between DM particles. This non-perturbative quantum effect arises from the contributions of ladder diagrams due to the exchange of new bosons between two incoming DM particles in the annihilation process. It leads to a velocity dependent annihilation cross section. When the relative velocity of the two particles is high enough, the Sommerfeld enhancement effect becomes negligible. Therefore at the early stage of the Universe, the cross section keeps to be a relatively low value which can give the right relic density. When the DM particles cool down significantly today, a larger annihilation cross section can be obtained. There are several works employing the Sommerfeld effect to explain the large BF as implied by the CR lepton data (e.g. [194, 211–213]).

In the literature, the Sommerfeld enhancement has been discussed for $\chi\chi\to W^+W^-$ if $W^\pm$ is light enough

compared to heavy DM with mass of several TeV [194, 214]. However, the W boson may over-produce antiprotons and be conflict with the PAMELA data. If the mediator ϕ boson is light enough instead, e.g. $m_\phi \leqslant O(1)$GeV, the production of antiprotons will be kinematically suppressed [211, 212, 215, 216]. Therefore the existence of light boson interpreters the PAMELA results elegantly.

However, further analysis finds that the enhancement of cross section due to the Sommerfeld effect would also affect the thermal history of DM in the early Universe. The calculation of DM relic density with Sommerfeld enhancement depends on several issues, such as the temperature of kinematic decoupling [217–219] and the efficiency of self-interactions for persevering thermal velocity distribution [219]. Detailed calculation shows there is a tension between large enhancement factor and correct DM relic density [219, 220]. In order to obtain correct DM relic density for $m_\chi \sim$1 TeV and $m_\phi \sim 1$ GeV, the maximal value of enhancement factor S for $\chi\chi \to \phi\phi \to \mu^+\mu^-\mu^+\mu^-$ is only $\sim O(10^2)$ which is smaller than the required value $O(10^3)$. In [221] the decay channel of $\phi \to e^+e^-$ is considered and a special configuration of "dark sector" is assumed, which can relax the constraint on the maximal BF.

The light mediator, a scalar or a vector boson, can interact with leptons via the small mixing with the Higgs boson or gauge boson in the SM. This kind of interactions is called "dark force" in the literature. The small mixing can be achieved by intergrading out some heavy fields which interact with both ϕ boson and SM boson, and induce small mass of ϕ as $m_\phi \sim 10^{-3} m_\chi$ naturally [222, 223]. The light mediators may be produced by the collisions between electrons and/or protons, and can be tested at the "fixed target" experiments [224–226], low-energy electron-positron colliders [227–229] or high-energy hadron colliders [230, 231].

4.4.5 Decaying dark matter

The final way to solve the discrepancy between the early annihilation rate and today's lepton generation rate is to assume that leptons are generated by DM decay. Therefore the decay process dominates over the annihilation process today. BF is not needed in such scenario obviously.

If there exists some tiny symmetry violation, the DM particles may decay very slowly to SM particles. Since the decay of DM should not reduce the abundance of DM in the universe significantly, the lifetime of DM should be much longer than the age of the universe $\sim 10^{17}$ s. If DM particles can decay into electrons or muons via some leptonic interactions, the flux of positron excess can be interpreted by the decaying DM with lifetime of $\sim O(10^{26})$ s [191, 232–236]. Such long lifetime of DM can be derived naturally by some high energy scale suppressed operators [237]. For instance, if a DM particle with a mass of 1 TeV decays via dimension 6 operators, its lifetime would be $\tau \sim 8\pi\Lambda^4_{GUT}/m^5_\chi \sim 3 \times 10^{27}$ s. The signatures of high energy photons [238–244] and neutrinos [245, 246] from decaying DM have been widely studied in the literature.

Note that the fluxes of high energy photons and neutrinos induced by decaying DM and annihilating DM are proportional to the DM number density and the square of DM number density, respectively. Such features can be used to distinguish different DM scenarios.

4.5 Discrimination between astrophysical and dark matter scenarios

As we discussed above, all the explanations to the positron/electron excesses fall into two categories: the astrophysical origin and the DM origin. An important question is if we can discriminate the two kinds of origins.

First we should state that by the local observation it is impossible to distinguish the decaying and annihilation DM scenarios [247]. This is easy to understand. The final states of the decay and annihilation are the same. The only difference comes from the source distribution of positrons from DM annihilation and decay. However, the observed high energy electron/positrons should come from local region near the solar system. This makes the two cases indistinguishable.

In Ref. [248] we try to see which scenario of the positrons between the astrophysical source and the DM is more favored by the present data. We assume pulsars as the typical astrophysical sources contributing to the positron excess, and compare the goodness of fit to the data with the DM scenario through a global fit method. The contribution of pulsars is parametrized with three new parameters, the power law index α, the cutoff energy E_c and the normalization $A_{\rm psr}$. For the DM case we fit the mass m_χ, cross section $\langle\sigma v\rangle$, and 4 branching ratios to leptons and quarks. The data include the PAMELA positron fraction, the PAMELA electron spectrum [154], Fermi-LAT total electron spectrum [158], and HESS total electron spectrum [156, 157]. The fitting parameters are given in Table 2 and the best fitting results compared with the data are shown in Fig. 12. We see that when including either pulsar or DM the fitting is improved essentially compared with the pure background fitting. However, the χ^2/d.o.f. for the pulsar and DM scenarios are almost the same. That is to say we cannot

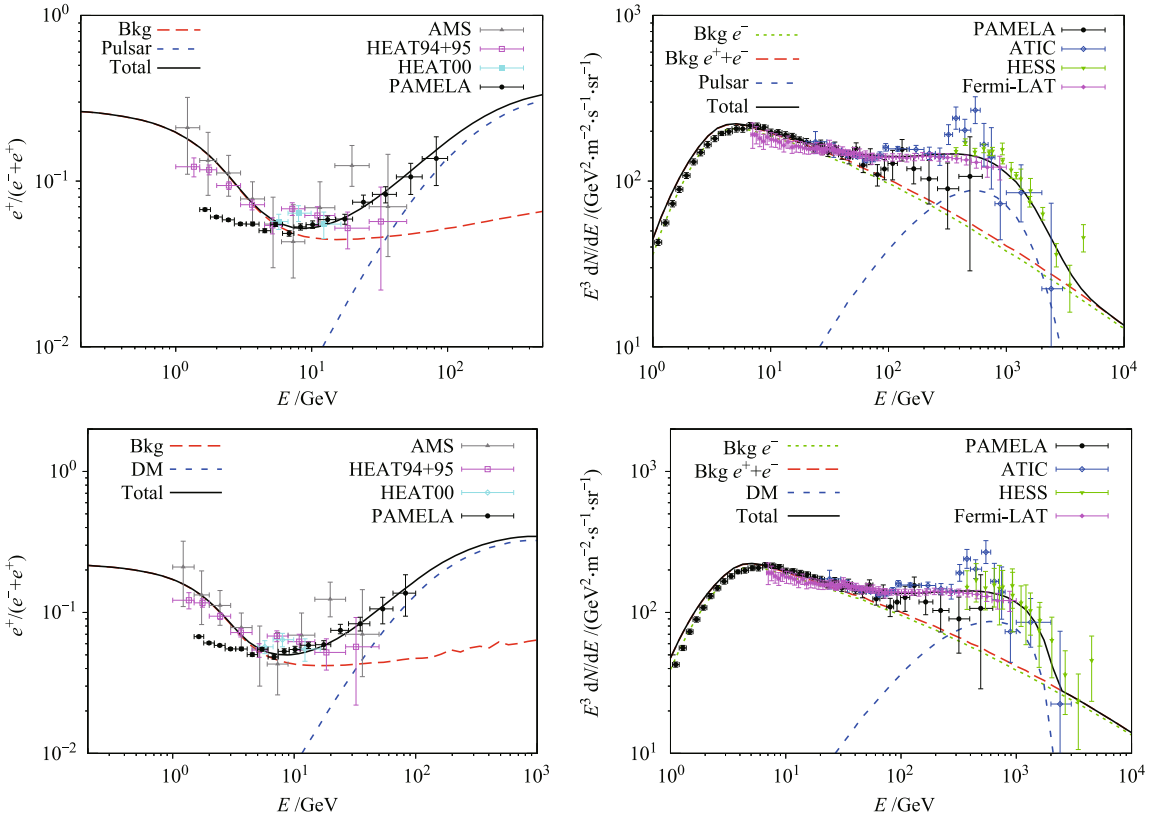

Fig. 12 Best-fit positron fraction (*left*) and electron spectra (*right*) for the scenarios with pulsars (*top panels*) and DM annihilation (*bottom*) as the extra sources of positrons and electrons. Reproduced from Ref. [248].

Table 2 Fitting parameters with 1σ uncertainties or 2σ limits. Note that for the "bkg" case the reduced χ^2 is too large that the uncertainties of the parameters should not be statistically meaningful. Taken from Ref. [248].

	Bkg	Bkg+pulsar	Bkg+DM
γ_1	< 1.532(95% C.L.)	< 1.619(95% C.L.)	< 1.610(95% C.L.)
γ_2	2.557 ± 0.007	2.712 ± 0.014	2.706 ± 0.013
$\log(A_{\rm Bkg})^{\rm a)}$	-8.959 ± 0.003	-8.997 ± 0.007	-8.997 ± 0.006
$E_{\rm br}$/GeV	$3.599^{+0.123}_{-0.112}$	$4.254^{+0.278}_{-0.287}$	$4.283^{+0.246}_{-0.259}$
ϕ/GV	0.324 ± 0.016	0.383 ± 0.042	0.371 ± 0.037
c_{e^+}	1.462 ± 0.035	$1.438^{+0.076}_{-0.079}$	1.394 ± 0.053
$c_{\bar{p}}$	1.194 ± 0.039	1.225 ± 0.043	1.210 ± 0.045
$\log(A_{\rm psr})^{\rm a)}$	—	$-27.923^{+0.534}_{-0.537}$	—
α	—	1.284 ± 0.104	—
E_c/TeV	—	$0.861^{+0.170}_{-0.164}$	—
m_χ/TeV	—	—	$2.341^{+0.492}_{-0.391}$
$\log[\sigma v(\rm cm^3 \cdot s^{-1})]$	—	—	-22.34 ± 0.13
B_e	—	—	< 0.379(95% C.L.)
B_μ	—	—	< 0.334(95% C.L.)
B_τ	—	—	$0.713^{+0.141}_{-0.152}$
B_u	—	—	< 0.005(95% C.L.)
χ^2/d.o.f	3.390	1.047	1.078

[a)] In unit of $\rm cm^{-2} \cdot sr^{-1} \cdot s^{-1} \cdot MeV^{-1}$.

distinguish the two scenarios according to the present electron/positron data.

There are proposals to distinguish these two scenarios with future experiments. In Ref. [249] the authors considered three cases to fit the ATIC data: the nearby pulsars, DM annihilation into W boson pair and Kaluza–

Klein DM that produce a sharp cutoff. The three models give different electron spectra, especially around the cutoff, as shown in Fig. 13. They proposed to distinguish the different scenarios by the IACTs, such as HESS, VERITAS and MAGIC.

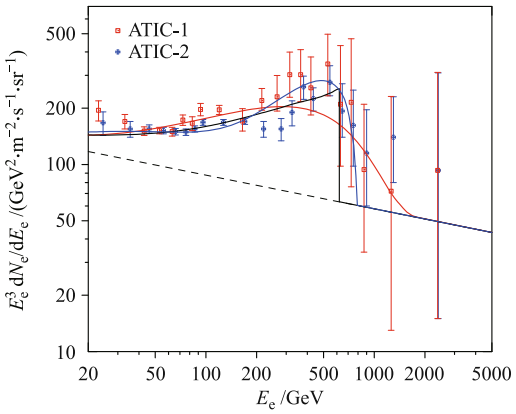

Fig. 13 The spectrum predicted from three possible sources: a nearby pulsar (*red*), annihilation to W^+W^- from 800 GeV DM (*blue*), and annihilation of 620 GeV Kaluza–Klein DM (which annihilates to e^+e^-, $\mu^+\mu^-$, and $\tau^+\tau^-$ with branching ratios 20% each, black). Reproduced from Ref. [249].

In Ref. [171] the authors studied the pulsar contribution to the electron/positron spectrum. They pointed out that at higher energies the spectrum is dominated by a few young nearby pulsars, which therefore induces wiggle-like features. If the electron/positron spectrum can be measured with much higher precision and the wiggle-like features are detected it will strongly favor the pulsar origin of the positron/electron excesses.

At present the most important experiment for DM indirect detection is certainly the AMS02 [250]. The AMS02 has accumulated data for nearly two years. The AMS02 will measure the CR spectra with much higher precision than the present data, which will reduce the uncertainties of background model significantly. It is possible that AMS02 will make breakthroughs in the indirect detection of DM. In Refs. [251, 252] the potential of AMS02 to measure the positron spectrum and the possibility to distinguish different kinds of the extra sources were discussed.

A new satellite experiment has been proposed in China, which is called Dark Matter Particle Explorer (DAMPE) [253]. DAMPE is an electromagnetic calorimeter dedicated to measure the electron+positron with energies from about 5 GeV up to about 10 TeV. With the large effective area of $\sim 0.36\,\mathrm{m}^2$, DAMPE could measure the total electron+positron spectra with high precision. This will test the prediction of the wiggle-like features in Ref. [171]. An important goal of DAMPE is to measure the shape of the cutoff of electron spectrum and try to distinguish different scenarios to explain the positron/electron excesses.

Another widely used way to discriminate different models is the photon emission [254–267]. In Ref. [268] we discuss the difference of the synchrotron and inverse Compton (IC) radiation from the Galactic center region for the pulsar, DM annihilation and DM decay scenarios. The key point is that the three scenarios have very different spatial distribution and the largest difference is at the Galactic center. All the scenarios can explain well the local observation by adjusting the parameters. However, once they are normalized at the position of the Earth they should show great difference at the Galactic center. Since the electrons/positrons can not propagate to the Earth due to fast energy loss we propose to observe the difference by their synchrotron and IC radiation.

Figure 14 shows the calculated synchrotron emission (top) and IC γ-ray spectrum (bottom) in the inner

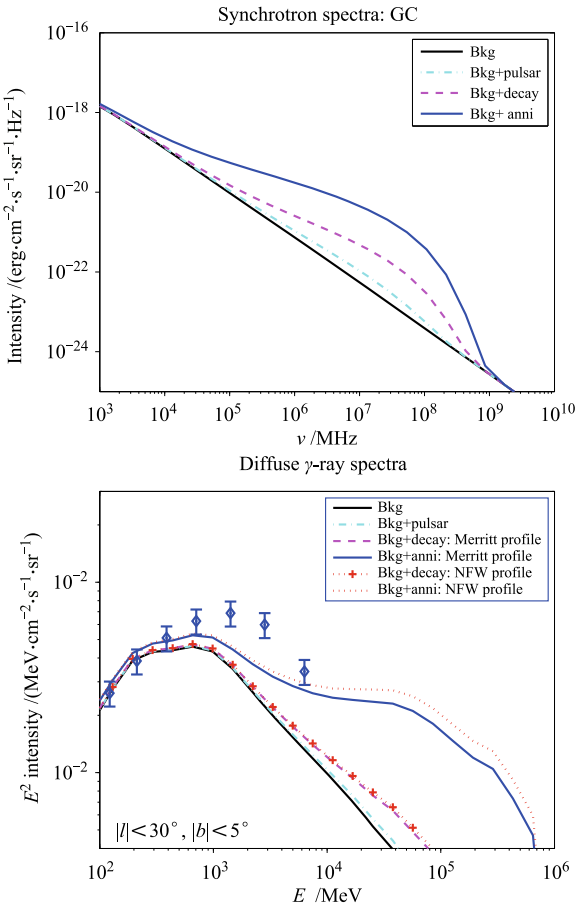

Fig. 14 *Upper*: The average synchrotron spectra of the three scenarios within a bin size of 20° × 20° around Galactic center; *Lower*: The contributions to the diffuse γ-ray spectra in the region $|l| < 30°, |b| < 5°$ for the three scenarios, compared with the EGRET data [269]. Reproduced from Ref. [268].

Galaxy. In this calculation the DM density profile is adopted to be the Einasto profile [270]. We can see that the three scenarios indeed show great difference at the inner galaxy region. Here we take a large region around the Galactic center is mainly due to the large uncertainties of the DM density profile. We also considered the cases for NFW or cored isothermal profiles. We find even for the cored isothermal profile the radiation spectra still show distinguishable differences.

5 Status of indirect detection – gamma rays

Gamma-ray photons are better than the charged CRs for the indirect search of DM due to the simple propagation. By means of γ-rays we can trace back to the sites where DM concentrates and map the distribution of DM. The energy spectrum of γ-rays is less affected during the propagation (except for high redshift sources) and could directly reflect the properties of DM particles. Furthermore, the photons can enlarge the detection range of DM significantly compared with the charged CRs which are almost limited in the Milky Way.

There are in general two ways to produce photons from the DM: the *primary* emission radiated directly from the DM annihilation/decay or from the decay of the final state particles, and the *secondary* emission produced through the inverse Compton scattering, synchrotron radiation or bremsstrahlung radiation of the DM-induced particles (mainly electrons and positrons). For WIMPs, the photon emission is mainly at the γ-ray band, with some kind of *secondary* emission such as the synchrotron radiation covering from X-ray to radio bands. In this review we focus on the recent progress in γ-ray search of DM.

Fermi space telescope is one of the most important facilities in operation for the γ-ray detection. The sensitivity of searching for DM with Fermi is up to now the highest for the general WIMP models. There are also ground-based VHE γ-ray detectors such as the imaging atmospheric Cerenkov telescopes (e.g., HESS, VERITAS and MAGIC) and air shower array detectors (e.g., ARGO-YBJ), which could be specifically powerful for heavy DM (m_χ ~TeV).

5.1 Fermi

5.1.1 Dwarf galaxies

The Milky Way dwarf galaxies are ideal laboratories for the indirect detection of DM. The dwarf galaxies are DM dominated with mass-to-light ratio of the order 10^2–10^3 [271]. The lack of gas content makes it free of γ-ray emission, resulting in a clean target for the search of DM signal. There are many works using the Fermi-LAT data to search for DM signal or constrain the DM model parameters [97, 272–276].

Using the first 11 month data of dwarf galaxies, the Fermi-LAT collaboration found no indication of γ-ray emission from these objects and strong constraints on the DM annihilation cross section were given [272]. With accumulation of the exposure, the limits were significantly improved, through additionally a joint analysis of many dwarf galaxies by Fermi-LAT collaboration and others [97, 273]. Figure 15 shows the 95% confidence level upper limits on the cross section $\langle\sigma v\rangle$ for selected annihilation channels derived in [97]. In such an analysis, the uncertainty of the DM density distribution in individual dwarf galaxy is also taken into account in the likelihood fitting. It is shown that for DM with mass less than ~ 30 GeV and annihilation channels $b\bar{b}$ and $\tau^+\tau^-$, the generic cross section of WIMPs which were thermally produced in the early Universe and match the correct relic density, $\langle\sigma v\rangle \sim 3\times10^{-26}$ cm^3 s^{-1}, can be ruled out by the γ-ray observations.

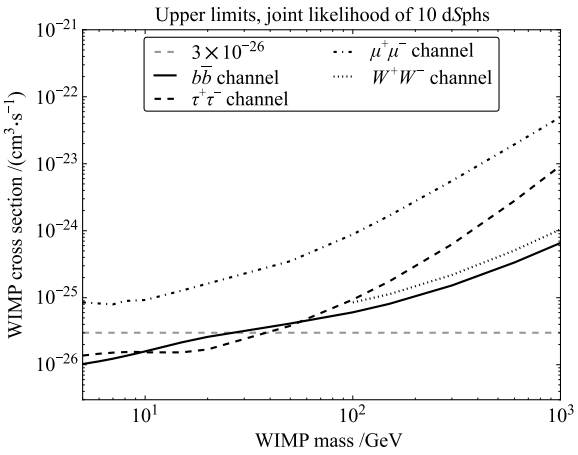

Fig. 15 Fermi 95% confidence level upper limits on WIMP annihilation cross section for $b\bar{b}$, W^+W^-, $\mu^+\mu^-$ and $\tau^+\tau^-$ channels which induce continuous γ-ray spectra. Reproduced from Ref. [97].

In Ref. [277] an update of the constraints to the 4-year Fermi-LAT data was given. In this analysis, a DM model-independent likelihood map, on the "$E_{\rm bin}$−flux" plane, of the Fermi-LAT data was derived through binning the data in multiple energy bins. Then the total likelihood of any "signal" spectrum can be easily obtained with the likelihood map. This method was tested to give

[7] http://fermi.gsfc.nasa.gov/ssc/data/analysis/software/

consistent results with that done using the Fermi Scientific Tool[7] (same as in Ref. [97]). It was found that the 4-year result [277] was comparable with the 2-year one [97] shown above for $m_\chi \lesssim 20$ GeV and even weaker by a factor of 2–3 for higher mass DM particles. Similar conclusion was also reported recently in the Fermi international Symposium [278]. Such a result could be due to the statistical fluctuations and different event classifications in those analyses [278]. In addition the photon yield spectrum also have a factor of 2–3 difference between different simulation codes [279–281]. Finally, the substructures in the dwarf galaxies, although generally not important, would contribute a factor of several to the uncertainty based on the numerical simulation [282]. Therefore we should keep in mind that the uncertainty of the constraints from γ-ray observations of dwarf galaxies, in spite that it is less affected by the DM density profile [283], is still a factor of ~ 10.

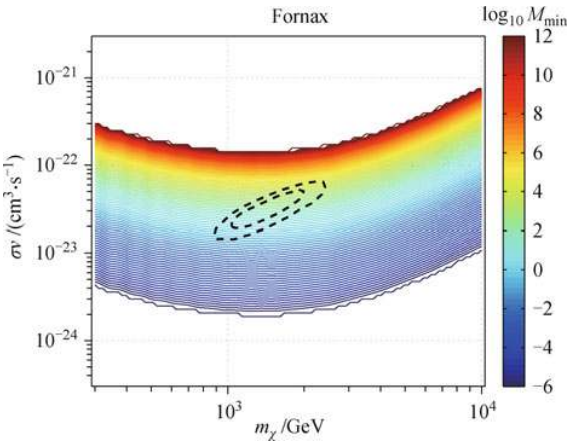

Fig. 16 The 95% upper limits of DM annihilation cross section to $\mu^+\mu$ from Fermi-LAT observations of galaxy cluster Fornax. Different colors show the results for different values of the minimal subhalo mass. The circles show the "required" parameter region to fit the Milky Way $e^\pm$ excesses [238]. Reproduced from Ref. [267].

5.1.2 *Galaxy clusters*

Galaxy clusters are another good type of targets to search for DM signal. There is currently no γ-ray emission found from galaxy clusters, and stringent limits on the γ-ray emission were set by Fermi-LAT [284]. Due to the low background emission and the large amount of DM, galaxy clusters can also give effective constraints on the DM model parameters [243, 267, 285–292].

For the DM annihilation in the galaxy clusters, a large uncertainty comes from the substructures in the clusters. We know there are substructures at least down to the mass scale of dwarf galaxies, but it is not clear whether the substructures can be extrapolated down to very low masses (e.g., $10^{-6}\ M_\odot$ as expected for typical CDM) which are beyond the resolution limit of observations and numerical simulations. Based on the direct extrapolation of simulation results of CDM, the boost factor arises from substructures for typical clusters can reach 10^3 with significant variation for cutoff mass $10^{-6}\ M_\odot$ [282]. Figure 16 illustrates the uncertainties of the constraints on DM models from substructures [267]. With conservative consideration of the substructures down to dwarf galaxy mass, the constraint on DM annihilation cross section is weaker than that derived from dwarf galaxies [285].

Another issue of searching for DM signal from galaxy clusters is that the targets should be taken as extended sources. For some nearby clusters, the virial radii reach several degrees, well beyond the resolution angle of Fermi-LAT detector for $E >$GeV. In [293] it was found that the spatial extension of the clusters would play a crucial role in searching for the potential signals. A marginal detection of extended γ-ray emission from Virgo cluster was found assuming a spatial template of DM annihilation with significant boost of substructures [293]. Although it was then suggested that new point sources which were not included in the Fermi catalog would contribute a fraction to the "signal" [292, 294], it is still necessary to pay attention to the spatial extension of the sources when doing similar searches.

Finally we comment that the galaxy clusters are powerful to probe decaying DM [243, 286, 287, 290]. Since the γ-ray flux induced by decaying DM is proportional to the total mass of DM in the cluster, the uncertainty of the constraint on decaying DM scenario arising from the DM substructure model is much smaller, and robust results could be derived. It was shown that the constraint on the DM lifetime from galaxy clusters was generally stronger than that from dwarf galaxies and nearby galaxies [286].

5.1.3 *Star clusters*

The Milky Way globular clusters, defined as spherical ensembles of stars that orbit the Galaxy as satellites, are potential targets for the indirect detection of DM. Although observationally there is in general no significant amount of DM in the globular clusters [295–297], the adiabatic contraction process in the cosmological formation context [298] due to the infall of baryons will give birth to a high density spike of DM and can in principle result in a high annihilation rate of DM.

In Ref. [299] the authors used the Fermi-LAT data of two globular clusters, NGC 6388 and M 15 which favor the astrophysical origin, to search for the DM signals. Strong γ-ray emission from NGC 6388 was reported, which was generally thought to come from the popula-

tion of millisecond pulsars [300]. No γ-ray emission from M 15 was found. The constraints on the DM annihilation cross section were derived [299]. Compared with the constraints from dwarf galaxies, the globular clusters could give even stronger constraints. However, there are very large systematic uncertainties for such a study, from the hypothesis of the origin of the globular clusters, the interaction between DM and baryons during the cluster evolution and the modification of DM profile due to adiabatic growth of the intermediate mass black hole in the center of the clusters.

5.1.4 Galactic center

The advantage of the Galactic center as the target for γ-ray detection of DM is that it is nearby with expected high density of DM. Although the density profile in small region around the Galactic center is not clear, the average annihilation J-factor, which is defined as the line-of-sight integral of DM density square averaged within a solid angle, in a relatively large region of the Galactic center is generally much higher than those of dwarf galaxies and cluster of galaxies [97, 256, 285]. However, the disadvantage is that the Galactic center is a so complex astrophysical laboratory that the background γ-ray emission is very strong and far from a clear understanding. Thus the problem is to distinguish the potential signal, if any, from the background emission.

Through analyzing the Fermi data, one group reported the extended γ-ray excess in the Galactic center which could be consistent with a DM annihilation origin with mass 10s GeV [301–303]. Such a claim was confirmed by other groups with independent analyses[8] [304, 305]. Figure 17 shows the extracted spectrum of the extended γ-ray excess in the Galactic center and the required parameter region if DM annihilation is adopted to explain it [301]. The DM density profile is adopted to be a generic Navarro–Frenk–White (NFW, [306]) profile with inner slope $\alpha = 1.3$ in order to be consistent with the spatial distribution of the excess γ-rays. It is interesting to note that the mass of the DM particle, which is fitted to be about tens of GeV, may be consistent with the suspected signals from direct detection experiments DAMA/LIBRA [307], CoGeNT [24] and CRESST [25].

Nevertheless, because the Galactic center is so complicated, it is still very difficult to distinguish the DM scenario of such an excess from the potential astrophysical sources such as cosmic rays from the supermassive black hole [302, 303], or a population of millisecond pulsars [308]. It should be also cautious that the understanding of the diffuse background emission close to the Galactic center is poor and the contamination of the diffuse background to this excess is still possible.

Conservatively one can set upper limits on the DM model parameters with the observational data [301, 309–312]. For DM mass less than ~ 100 GeV, the upper limit of the annihilation cross section was found to be close to or lower than the natural value 3×10^{-26} cm^3·s^{-1} [301, 311]. Such a limit is at least comparable to that derived from other observations such as the dwarf galaxies.

5.1.5 Milky Way halo and subhalos

More works are trying to search for the DM signal from γ-ray observations of the Milky Way halo [239, 242, 262, 313–317], since the signal-to-noise ratio will be even higher in the halo than that in the Galactic center [318]. Furthermore, the result from the Milky Way halo is less sensitive to the DM density profile which is highly uncertain in the inner Galaxy. Using 2-year Fermi-LAT data of the whole Milky Way halo excluding the Galactic plane, the LAT collaboration derived constraints on the DM annihilation cross section or decay lifetime for a wide range of final states, conservatively through comparing the data with the expected signal from DM [316]. The constraints are relatively weak, however. With optimizing analysis regions, and improving diffuse backgrounds, the LAT collaboration updated the results and gave more stringent constraints on the DM model parameters [317]. The uncertainties of the astrophysical diffuse background which were poorly constrained, e.g., the diffusive halo height, the cosmic ray source distribution, the injection spectrum index of electrons, and the dust to gas ratio of the interstellar medium, were also taken into account using a profile likelihood method [317]. The results were found to be competitive with other probes like dwarf galaxies and galaxy clusters.

Subhalos are expected to widely exist in the Milky Way halo, in the CDM structure formation pattern. Less affected by the tidal stripping effect of the main halo, subhalos could be more abundant in the large halo away from the Galactic center. The dwarf galaxies are part of the subhalos in the Milky Way. Besides the dwarf galaxies we might expect the existence of DM-only subhalos which are not visible with current astronomical observations. Such DM-only subhalos could be γ-ray emitters if the flux is high enough [319, 320]. Several works tried to investigate the possible connection between the Fermi

[8] Note in Ref. [304] the conclusion was against the existence of the extra "signal" from DM annihilation, but in their analysis they did find that including an additional source consistent with DM annihilation the fit to the data was significantly improved.

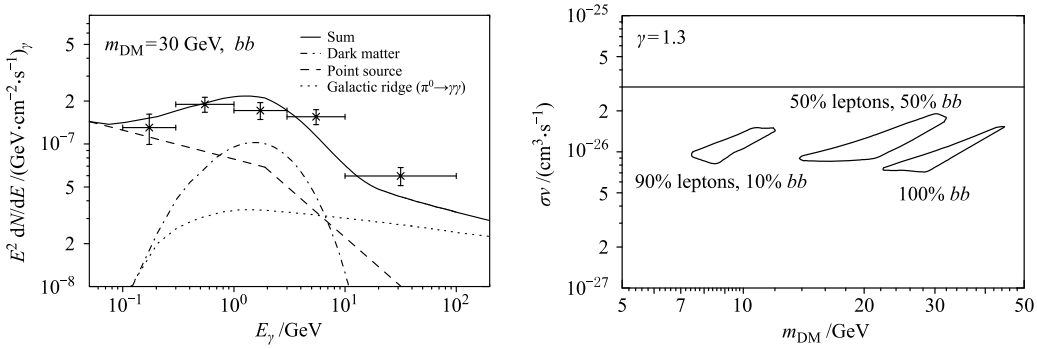

Fig. 17 *Left*: Spectrum of the excess γ-rays in the Galactic center and an illustration to employ a point source component, diffuse component from the Galactic ridge together with a DM component to explain the data. *Right*: Fitting parameter space for DM annihilation scenario to account for the excess for different assumptions of DM annihilation channels. Reproduced from Ref. [301].

unassociated sources and the DM subhalos [321–326]. The γ-ray emission from DM subhalos should be non-variable, spatially extended and spectrally hard. Applying these criteria to the unassociated Fermi sources, the LAT collaboration found that most of the sources did not pass the cuts, except two candidates [324]. However, further analyses identified the rest two sources to a pulsar and two active galactic nuclei respectively [324]. Such a result could be interpreted in the context of structure formation of the ΛCDM scenario. Using slightly different critera together with the multi-wavelength observations, another group reached a similar conclusion that no DM subhalo in the Fermi unassociated source catalog could be identified now [322, 325].

The population of low mass subhalos, unresolved in the current numerical simulations, could contribute to the diffuse γ-ray emission of DM annihilation in the halo [262, 327, 328]. The contribution of subhalos suffers from large uncertainties of the structure parameters extrapolated according to the numerical simulations. Roughly speaking for typical CDM scenario the boost factors of the γ-ray signal could be several to several tens, depending on the directions [328]. Thus the constraints from the Milky Way halo could be even stronger considering the contribution of subhalos.

Besides the flux of the γ-ray emission, the spatial morphology can also provide useful identification of the DM signals. This includes the large scale morphology [241, 329–332] and the statistical properties at small scales [333–339]. It was shown that even the DM annihilation contributed only a small fraction of the diffuse background, the anisotropy detection could have the potential to identify it from the background (e.g., [335]).

5.1.6 Extragalactic gamma-ray background

The extragalactic γ-ray background (EGRB) is a probe to explore the accumulation of the DM evolving in the whole history of the Universe. Measurement of the EGRB by Fermi-LAT showed a structureless power-law from 200 MeV to 100 GeV [340]. Most recently the analysis extended up to 400 GeV with result being basically consistent with the previous published one [341]. The DM model is in general difficult to produce such a single power-law spectrum in a very wide energy range. Therefore the EGRB is widely employed to constrain the DM model parameters [244, 266, 342–351].

The major uncertainty of the expectation of DM contribution to the EGRB flux is the clumpiness enhancement factor for annihilating DM scenario. For different assumptions of the density profile of each halo, the halo mass/luminosity function, the cutoff mass of the minimal halo and/or the concentration-mass relation, the clumpiness enhancement factor can differ by several orders of magnitude (e.g., [342]). The most conservative limits can barely reach some models interested in the community such as those proposed to explain the positron/electron excesses [342]. The EGRB has the potential to probe larger range of the parameter space, but it depends on more precise knowledge about the DM structure formation and the astrophysical contribution to the EGRB.

For decaying DM scenario, the constraints are more robust due to the less effect of structures [244, 344]. It was shown that the EGRB measured by Fermi-LAT could exclude almost all the parameter regions of DM models with two-body channels to account for the cosmic ray positron/electron excesses (Fig. 18, [244]). For other decaying channels such as $b\bar{b}$, the constraint from EGRB is also among the most stringent ones [244].

The statistical anisotropy of extragalactic DM annihilation may have distinct behavior from the astrophysical sources and can be used to detect the DM signal

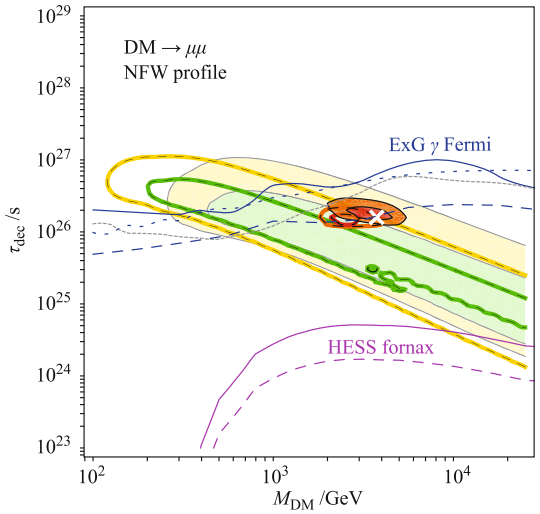

Fig. 18 Constraints on the DM lifetime with Fermi EGRB data and HESS observation of galaxy cluster Draco. Reproduced from Ref. [244].

from EGRB [352–354]. It was proposed that the energy dependence of the anisotropy of EGRB could be another interesting observable which might be more sensitive to identify the DM signal [355–357]. With the intensity and anisotropy energy spectra, different components of the diffuse background can be decomposed model-independently [357]. A positive detection of the angular power for $155 \leqslant l \leqslant 504$ with Fermi-LAT data was reported [358]. The measured angular power is approximately independent with scale l, which implies that it originates from the contribution of one or more unclustered source populations. Furthermore, the lack of strong energy dependence of the amplitude of the angular power normalized to the mean intensity in each energy bin indicates that a single source class may dominate the contribution to the anisotropy and it provides a constant fraction to the intensity of the EGRB [358]. The result is consistent with the blazar origin of the EGRB [358], which implies the lack of a signal from DM.

5.1.7 Line emission

The monochromatic γ-ray emission is usually called as the "smoking gun" diagnostic of the DM signal [359–363]. The DM particles may annihilate into a pair of photons or a photon plus another gauge boson or Higgs boson, resulting quasi-monochromatic γ-ray emissions. In addition the internal bremsstrahlung photons produced when DM annihilating into charged particles can also give prominent spectral features which will mimic the line emission [364–367].

With the purpose of searching for sharp spectral features, one group found a weak indication of the "signal" around $\sim$ 130 GeV in the public Fermi-LAT data with global significance $\sim 3\sigma$, which may be consistent with either an internal bremsstrahlung like signal or a γ-ray line [368, 369]. This "signal" was confirmed in the following studies [370, 371], and the significance could become higher if a $\sim 1.5^\circ$ offset of the "signal" region to the Galactic center was included [371]. The basic features of the tentative "signal" are:

- Spatially: extended; concentrated in the Galactic center with peak position slightly offset from the central supermassive black hole; consistent with Einasto or cuspy NFW (inner slope $\alpha \approx 1.2$) profile.
- Spectrally: sharp feature at $\sim$ 130 GeV with no significant spread; possibly a second line at $\sim$ 111 GeV; sharper for larger incidence angle events whose energy resolution is higher.

Figure 19 shows the spatial and spectral results of the line emission derived in Ref. [371].

Note there are still some discrepancies of the results of both the spatial and spectral properties. The spatial distribution of the 120–140 GeV photons was found elsewhere other than the Galactic center, with lower significance [370, 372]. Similar spectral features at other energies along the Galactic plane were also shown [372]. The most recent results reported by the LAT collaboration, with improvement of the energy resolution and reprocessed data with corrected energy scale, confirmed these complex features and found lower global significance $< 2\sigma$ of the "signal" around 135 GeV [373].

It was further reported that there might be another hint of 130 GeV line emission from the accumulation of data from several nearby galaxy clusters [374]. However, the arrival directions of the photons with highest significance are within 5° or 6° cone around each cluster, which are beyond the virial radii of all these clusters. The likelihood fit based on the DM density profile (together with substructures) of each cluster actually found no significant signal [311]. The analysis of dwarf galaxies showed no signal of line emission either [375].

The analysis of the unassociated sources in the second Fermi-LAT catalog (2FGL, [376]) suggested a local $\sim 3\sigma$ evidence of the existence of double line with energies consistent with that found in the inner Galaxy [377]. However, the overall γ-ray spectra of most of these unassociated sources which have potential line photons show distinct shape from that expected from DM annihilation [378]. It turns out that most of those unassociated sources should not be DM subhalos. Another independent study argued that the double lines from unas-

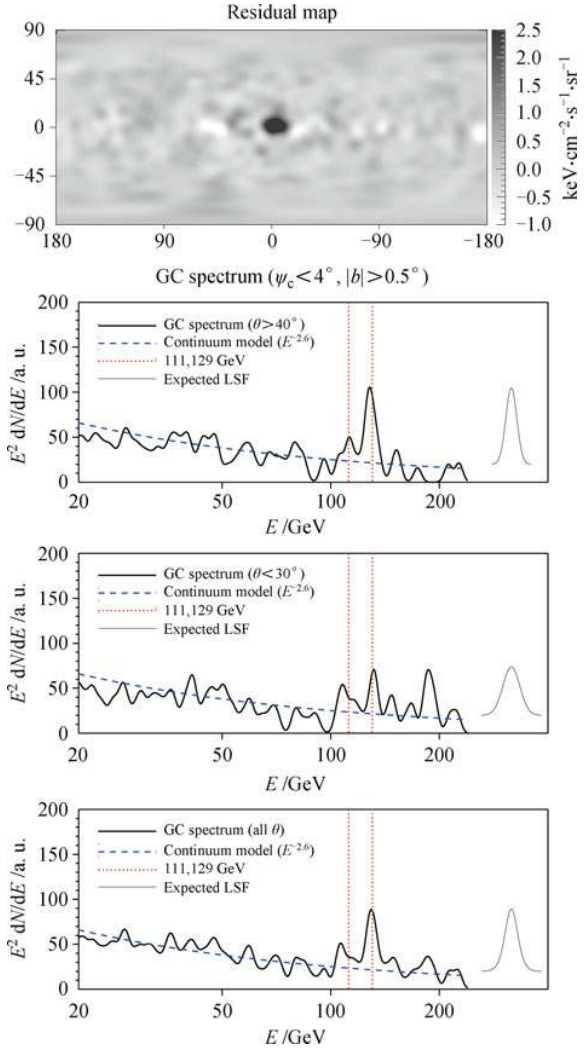

Fig. 19 *Upper*: The residual map of 120–140 GeV photons with subtraction of the maps of nearby energies: 80–100 GeV, 100–120 GeV, 140–160 GeV and 160–180 GeV. *Lower three panels*: Spectra of the emission within 4° of the cusp center $(l, b) = (-1.5°, 0)$ excluding $|b| < 0.5°$, for large incidence angle (*second*), small incidence angle (*third*) and total events (*bottom*). Reproduced from Ref. [371].

sociated sources could not be identified in the present statistics and energy resolution of Fermi-LAT and the "signal" should be an artifact of the applied selection criteria [379].

It is very important to consider the possible instrument systematics of this line "signal" [380–382]. The detailed study with currently available information of the detectors showed no systematical differences between the 130 GeV photons and photons with other energies [380]. The photons from the Galactic center region also show no systematical differences from those of other sky regions [382]. A marginally significant line feature at $E \sim 130$ GeV in the photons of the Earth limb, which is produced by the collisions between cosmic rays and the atmosphere, was found within a limited range of detector incidence angles [373, 381, 382]. Such a result raises concerns about the line signal found in the inner Galaxy. However, it is not easy to be understood with any plausible cause of the instrument behavior [382].

Described above are the current observational status of the 130 GeV line emission. We are not clear whether it is real or not at present from the Fermi-LAT data only. Nevertheless, there are many discussions on the theoretical implication of such a line in the sky, most of which focus on the DM models [383–417]. If DM annihilation is responsible for the line "signal", the required annihilation cross section is estimated to be $\sim 10^{-27}$ cm^3·s^{-1} for NFW or Einasto profile [369]. Such a cross section seems too large for typical DM annihilation into a pair of photons through a loop, due to the lack of strong continuous γ-ray emission as expected from the tree level contribution [311, 418–420]. On the other hand if the tree level annihilation is suppressed or forbidden, then we may need to finely tune the model parameters to reconcile with the relic density of DM [392, 399]. Other studies to constrain the DM models of the monochromatic line emission include the electron/positron spectra [421], radio data [422] and antiprotons [423]. Note that these constraints are not directly applicable on the line emission.

The offset of the γ-ray peak from the central black hole serves another challenge to the DM interpretation. However, in the case of low statistics, the fluctuation could naturally explain such an offset [424, 425]. Numerical simulation also suggest that an offset of several hundred parsec is generally plausible [426]. Note in [427] it was pointed out that the density cusp of DM could not survive the tidal force of the Milky Way given an off set of $\sim 1.5°$. A caveat is that the above estimate is based on the assumption of static equilibrium of the DM density profile.

Due to the potential importance of the γ-ray line for physics and astrophysics, it is very important to test it with other independent measurements. The currently operating experiment on the ISS, AMS02, can measure the electrons and photons up to TeV with an energy resolution of 2%–3% [250]. There is another on-going mission, CALorimetric Electron Telescope (CALET), which is planned to be placed on the ISS around 2014, has an energy resolution of 2% for photons with energies higher than 100 GeV [428]. The geometry factors of AMS02 and CALET for photons are much smaller than that of Fermi-LAT, and it will need much longer time to have enough statistics to test the line emission. A Chinese spatial

mission called DArk Matter Particle Explorer (DAMPE) which is planned to be launched in 2015, may have large enough geometry factor (~ 0.6 m^2 sr) and high enough energy resolution (1%–1.5% at 100 GeV) [253]. It is possible for DAMPE to test this line emission with one to two year operation [429]. A recently available test may come from the ground based Cerenkov telescopes HESS II [430]. For 50 hour exposure of the Galactic center region by HESS II a 5σ detection of the Fermi-LAT 130 GeV line can be reached [431]. The detectability or exclusion power will be much higher for the Cerenkov Telescope Array (CTA, [432]) project [431].

5.2 Ground based telescopes

In this subsection we briefly compile the results (limits) of DM searches with the ground based VHE γ-ray detectors, especially from Cerenkov telescopes. The threshold detection energy of the ground based atmospheric Cerenkov telescopes is about tens to hundreds GeV, and they are most sensitive for TeV photons. Therefore it will be more effective to probe the heavy DM using the ground based telescopes.

The search for DM signal has been carried out by Whipple [433], HESS [434–439], MAGIC [440, 441] and VERITAS [442]. The primary search targets are dwarf galaxies. Up to now no γ-ray emission was found from the dwarf galaxies, even for the very deep observations, and stringent upper limits of the γ-ray emission could be set [434, 436, 437, 440–442]. The upper limit of the DM annihilation cross section derived by the Cerenkov telescopes can reach 10^{-24} cm^3·s^{-1} for neutralino DM [434], and will be better than that given by Fermi-LAT for $m_\chi >$TeV. Better constraint comes from the observations of the Galactic center region [438]. However, the uncertainty from the density profile becomes larger.

The future experiment CTA will improve the sensitivity of VHE γ-ray detection by an order of magnitude compared with the current Cerenkov telescope arrays. It is expected to significantly improve the capability of searching for heavy DM [443].

6 Status of indirect detection – neutrinos

6.1 High energy neutrino telescopes

Unlike other products induced by DM, neutrinos have less trajectory defection and energy loss during the propagation due to the weak interaction. Therefore neutrinos may carry the information of the property and distribution of DM. For the same reason, neutrinos are more difficult to be detected compared with charged particles and photons. For a review of the high energy neutrino telescopes, see Ref. [444].

Neutrinos can only be observed indirectly through the charged leptons induced by neutrinos interacting with nuclei inside/outside the detector. These secondary leptons, such as electrons or muons, with high energy will emit Cerenkov radiation when they penetrate in the detector. Since the secondary lepton carries almost all the energy of neutrino and only has small trajectory defection from the original direction of neutrino, the information of neutrino can be well reconstructed via the Cerenkov emissions. The telescope can also detect the cascade showers induced by electron neutrinos and tau neutrinos, and by neutrino-nucleon scatterings via neutral current interactions [445]. However, the efficiency of such detection is much lower than detecting Cerenkov emissions.

The high energy neutrino telescopes, such as Super-Kamiokande (Super-K) [446], ANTARES [447] and IceCube [448, 449], are located in the deep underground, water and ice to be shielded from high energy cosmic ray backgrounds. The water or ice can be used as Cerenkov radiator for high energy muons. In order to improve the detection capability, the volume of telescope should be very large. Because high energy muons can propagate a long distance, the telescope may observe the muons produced outside the detector. Such effect enlarges the effective volume of the detector. For the same reason, in order to reduce high energy atmospheric muon background, the telescope observes the up-going muons induced by the up-going neutrinos which travel through the earth.

The final muon event rate at the detector can be given by Ref. [450] (for the calculation considering the energy dependent muon flux, see Refs. [451, 452])

$$\phi_\mu \simeq \int_{E_{th}}^{m_\chi} \mathrm{d}E_\mu \int \mathrm{d}E_{\nu_\mu} \frac{\mathrm{d}N_{\nu_\mu}}{\mathrm{d}E_{\nu_\mu}} \left(\frac{\mathrm{d}\sigma_{cc}^{\nu p}}{\mathrm{d}E_{\nu_\mu}} n_p + \frac{\mathrm{d}\sigma_{cc}^{\nu n}}{\mathrm{d}E_{\nu_\mu}} n_n \right) \times (R(E_\mu) + L) A_{eff} + (\nu \to \bar{\nu}) \quad (4)$$

where $n_p(n_n)$ is the number density of protons(neutrons) in matter around the detector, the muon range $R(E_\mu)$ denotes the distance that a muon could travel in matter before its energy drops below the detector's threshold energy E_{th}, L is the depth of the detector, A_{eff} is the detector's effective area for muons which depends on the muon energy, the notation $(\nu \to \bar{\nu})$ denotes that the anti-neutrino flux is also taken into account. $\mathrm{d}\sigma_{cc}^{\nu p}/\mathrm{d}E_\mu$ is the the cross section of deep inelastic neutrino-nucleon scattering which produces muons via charged current interactions. $\mathrm{d}N_{\nu_\mu}/\mathrm{d}E_{\nu_\mu}$ is the flux of the neutrinos induced

by DM.

The irreducible backgrounds are the up-going atmospheric neutrinos which are produced by the cosmic rays interacting with nuclei in the atmosphere [453]. In fact, almost all the high energy neutrinos observed at the neutrino telescopes are atmospheric neutrinos [454]. The atmospheric neutrinos are almost isotropic, while the neutrinos from DM are produced from particular direction. The flux of atmospheric neutrinos decreases as $\sim E_\nu^{-3.7}$, while the neutrinos from DM may have a harder spectrum. Therefore, high angular and energy resolutions of the telescope are essential to extract the signals from the smooth backgrounds.

6.2 Solar neutrinos from DM

When DM particles travel through a massive astrophysical object, such as the Sun (Earth), they may be gravitationally trapped and continuously lose energy by collisions with nuclei [455, 456]. Once captured, DM particles may have large annihilation rate due to high number density [457]. The time evolution of the DM population in the Sun can be given by

$$\dot{N} = C_\odot - C_A N^2 - C_E N \tag{5}$$

where $C_\odot$ is the capture rate, C_A is the thermally averaged DM annihilation cross section per volume, C_E is the evaporation rate which is only significant for light DM. If the capture process and annihilation process reach equilibrium over a long time scale, the annihilation rate is determined by capture rate as $\Gamma = \frac{1}{2}C_\odot$. The capture rate can be approximately given by Ref. [458] (general discussions of DM capture rate for the Earth and the Sun can be found in Refs. [16, 452, 459, 460])

$$C_\odot \sim 10^{20}\mathrm{s}^{-1}\frac{\rho_\chi}{0.3\ \mathrm{GeV}\cdot\mathrm{cm}^{-3}}\left(\frac{270\ \mathrm{km}\cdot\mathrm{s}^{-1}}{\bar{v}}\right)^3 \times\left(\frac{100\ \mathrm{GeV}}{m_\chi}\right)^2\frac{\sigma_{SD}^{\chi H}+\sigma_{SI}^{\chi H}+\sum_i \xi_i\sigma^{\chi N_i}}{10^{-42}\mathrm{cm}^2} \tag{6}$$

where ρ_χ and $\bar{v}$ are the mass density and RMS velocity of DM in the solar system respectively. The contribution of the i-th nuclear species depends on the elastic scattering cross section between DM and the i-th nucleus $\sigma^{\chi N_i}$. It also depends on the mass fraction and distribution of the i-th nuclei in the Sun and the properties of the scattering which can be presented by a numerical factor ξ_i [16, 458]. Since the SI cross section between DM and nucleon has been stringent constrained by the direct detections, the most important contribution for the capture rate and thus for the annihilation rate may be from the SD scattering between the DM and hydrogen in the Sun (for the discussions of inelastic DM, see Refs. [460–462]).

If the products of DM annihilations are e^+e^- or $\mu^+\mu^-$, they will not contribute to neutrino signals. For muons, the reason is they always lose most of energy before decay in the center of the Sun. For annihilation channels into $\tau^+\tau^-$, W^+W^-, ZZ, $t\bar{t}$, they produce neutrinos via cascade decays and the neutrino spectra for such channels are hard. For quark channels, since neutrinos are induced via hadron decays after hadronization process, the neutrino spectra are soft. Moreover, the light mesons lose energy easily before decay, therefore the contributions from light quarks to the neutrino signals are always small.

The high energy neutrinos produced at the solar center will interact with the nuclei before they escape from the Sun. The effects include the neutral current interaction, the charged current interaction and tau neutrino ν_τ re-injection from secondary tau decays. The other important effects are neutrino oscillations including the vacuum mixing and the MSW matter effects. The comprehensive discussions can be found in Ref. [463–465].

The final neutrino flux arrived at the Earth is

$$\frac{\mathrm{d}N_\nu}{\mathrm{d}E_\nu} \simeq \frac{C_\odot}{2}\frac{1}{4\pi R_{SE}^2}\sum_i Br_i\left(\frac{\mathrm{d}N_\nu}{\mathrm{d}E_\nu}\right)_i \tag{7}$$

where i runs over all the DM annihilation channels contributing to neutrino signals with branching fractions Br_i, $\left(\frac{\mathrm{d}N_\nu}{\mathrm{d}E_\nu}\right)_i$ is the neutrino energy spectrum after propagation for the i-th channel, and R_{SE} is the Sun-Earth distance. In fact, the high energy solar neutrino detections search for the combinations of $\sigma^{\chi p}\cdot Br_i$.

Recently, IceCube reported the results of the high energy solar neutrinos with the 79-string configuration and 317 days running (Fig. 20) [448]. Since no events from the DM are confirmed, upper-limits are set on the SD and SI DM-proton scattering cross sections for DM masses in the range of 20–5000 GeV. In the analysis, two typical initial neutrino spectra from $b\bar{b}$ ("soft") and W^+W^- ("hard") channels with the branching fractions Br=1 are adopted. For the SI cross section, the limits given by IceCube are weaker than those from CDMS [53, 468] and XENON100 [469]. The most stringent limits for DM masses of $O(100)$ GeV and W^+W^- channel from IceCube have reached $10^{-43}\mathrm{cm}^2$. For the SD cross section, the most stringent limits are given by IceCube for DM masses above 35 GeV and W^+W^- channel. The strict limits for lower DM masses are set by superheated liquid experiments, such as PICASSO [33] and SIMPLE [34]. It is also worth noting that in a particular DM model, such as MSSM, the SD constraints set by IceCube can also exclude some parameter regions allowed by current CDMS and XENON100 results.

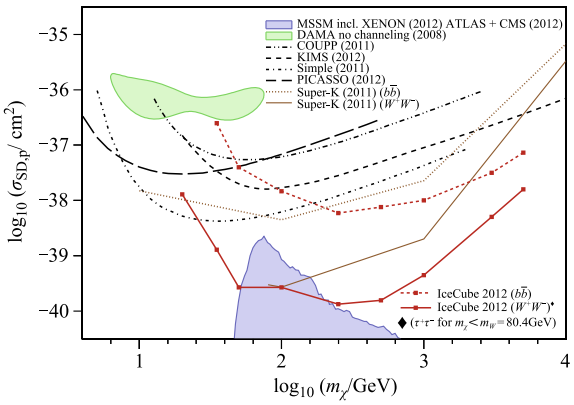

Fig. 20 Constraints on SD DM-nucleon scattering cross section for W^+W^- and $b\bar{b}$ annihilation channels by IceCube 79 strings. For comparison, other results from Super-K [446], DAMA [21, 36], COUPP [466], PICASSO [33], KIMS [22], SIMPLE [34], are also shown, together with the preferred regions in MSSM [467]. Reproduced from Ref. [448].

6.3 Cosmic neutrinos from DM

The DM annihilations or decays in the Galactic halo, Galactic Center(GC) [246, 470–472], subhalos [473, 474], dwarf satellite galaxies [475] and galaxy clusters [267, 476, 477] can produce high energy neutrinos. There are almost no astrophysical high energy neutrino sources in these regions which can mimic the DM signals. The flux of neutrinos observed at the earth can be given by (see e.g. [478])

$$\left(\frac{\mathrm{d}N_\nu}{\mathrm{d}E_\nu}\right)^A = \frac{1}{4\pi}\frac{\langle\sigma v\rangle}{2m_\chi^2} \times \left(\frac{\mathrm{d}N_\nu}{\mathrm{d}E_\nu}\right)_i^A \times J^A(\Delta\Omega) \quad (8)$$

$$\left(\frac{\mathrm{d}N_\nu}{\mathrm{d}E_\nu}\right)^D = \frac{1}{4\pi}\frac{1}{\tau_\chi m_\chi} \times \left(\frac{\mathrm{d}N_\nu}{\mathrm{d}E_\nu}\right)_i^D \times J^D(\Delta\Omega) \quad (9)$$

where the superscripts A and D denote annihilating and decaying DM respectively, τ_χ is the lifetime of decaying DM, $\left(\frac{\mathrm{d}N_\nu}{\mathrm{d}E_\nu}\right)_i$ is the initial neutrino energy spectrum. The J-factors J^A and J^D are the line-of-sight (l.o.s) integrals of the DM density ρ toward a direction of observation ψ integrated over a solid angle $\Delta\Omega$, which can be written as

$$J^A(\Delta\Omega) = \int \mathrm{d}\Omega \int_{l.o.s} \mathrm{d}l \;\; \rho^2[l(\psi)] \quad (10)$$

$$J^D(\Delta\Omega) = \int \mathrm{d}\Omega \int_{l.o.s} \mathrm{d}l \;\; \rho[l(\psi)] \quad (11)$$

The GC is the best object to search the neutrino signals due to the high density of DM. For IceCube located at the south pole, the neutrinos from the GC located in the southern sky are down-going. Although the down-going atmospheric muon background is very large, the IceCube collaboration has developed some techniques to reduce such background efficiently [449]. Since the cosmic muons enter the detector from outside, only the muon events which are produced inside the detector are selected. Due to the large volume of IceCube, the upper digital optical modules on each string and strings in the outer layer can be used to veto the atmospheric muons. Especially, the central strings of DeepCore with higher module density will use the surrounding IceCube detector as an active veto, and have strong capability to detect down-going neutrinos [479].

IceCube collaboration has reported the constraints on the neutrino signals from DM annihilations in the GC based on the performance of 40 strings during 367 days [449]. No data from DeepCore strings are used in this analysis. The main constraints are shown in Fig. 21. Since the neutrinos with higher energy are more easily reconstructed (due to large cross section and muon range) and suffer from smaller atmospheric neutrino background, the constraints for heavy DM are more stringent. If the dominant DM annihilation channel is $\nu\bar{\nu}$ (W^+W^-), the upper limit on the DM annihilation cross section for $m_\chi \sim 1$ TeV is $\sim 10^{-23}\mathrm{cm}^3\cdot\mathrm{s}^{-1}$($\sim 10^{-22}\mathrm{cm}^3\cdot\mathrm{s}^{-1}$). In the future, the IceCube with 79 strings and DeepCore will significantly improve these results due to larger volume and lower threshold.

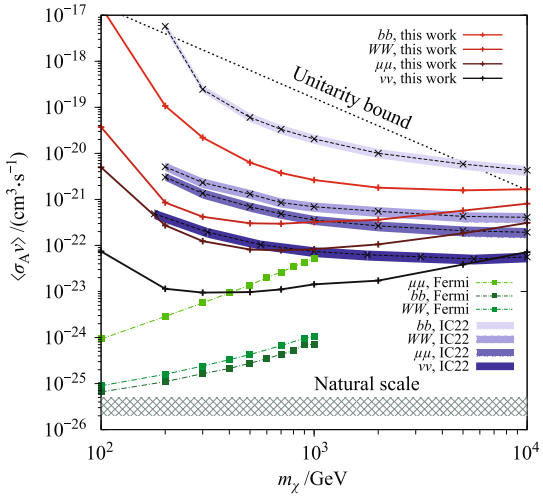

Fig. 21 Constraints on DM annihilation cross section for four channels by IceCube-40. For comparison, the results from the IceCube-22 outer Galactic halo analysis [480] and the Fermi-LAT dwarf galaxies observation [97] are also shown. Reproduced from Ref. [448].

Since the dwarf satellite galaxies and galaxy clusters are far away from the earth, the constraints for DM annihilation in these regions are weaker than the GC. For instance, for $m_\chi \sim 1$ TeV and W^+W^- channel, the upper-limit given by dwarf satellite galaxy searches on the DM

annihilation cross section is about $\sim 10^{-21}\mathrm{cm}^3\cdot\mathrm{s}^{-1}$ [481]. Note that the DM substructure models of e galaxy clusters have large uncertainties. The constraints on DM annihilation cross sections can be improved by some substructure models and parameter configurations [267].

7 Summary

The existence of DM has been firmly established for a long time by widely astronomical observations. To detect DM particle and study its properties is a fundamental problem in cosmology and particle physics. Extreme efforts have been paid for DM detection and great progresses have been achieved in recent years.

The direct detection experiments have been widely developed all over the world. The sensitivity was improved rapidly in last years. However, most experiments give null results and very strong constraints on the interaction strength between DM and nucleon have been given. DAMA, CoGeNT and CRESST have observed some anomalous events. Interpreting these events as DM signal will lead to inconsistency with other null results.

As the successful running of LHC, constraints on the nature of DM from collider data are derived. It is shown that the collider search is complementary to the direct detection. Especially for small DM mass the LHC gives very strong constraints while the direct detection sensitivity becomes worse as DM mass decreases.

The most important progress comes from the indirect detection. PAMELA, ATIC and Fermi all observed positron and electron excesses in cosmic rays. It is widely accepted that these data mean new sources contributing to primary positrons and electrons. Both astrophysical origins and DM origins are extensively studied in the literature. However, if the anomalies are interpreted by DM annihilation the DM property is highly non-trivial. Firstly, DM couples with leptons dominantly and the coupling with quarks should be suppressed. Secondly, the annihilation rate should be boosted with a very large BF at $O(10^3)$. Several mechanisms are proposed to give the large BF. However, later careful studies show those proposals can not work efficiently. The decay scenario is still working quite well. There are also many discussions trying to discriminate the astrophysical and DM scenarios.

The Fermi-LAT has made great success in γ-ray detection. However, all the observations are consistent with CR expectation and thus give strong constraints on the DM annihilation rate. Observations from dwarf galaxies, galaxy clusters, Galactic center and Galactic halo all lead to strong constraints on the DM annihilation rate. An interesting progress recently is that the line spectrum γ-ray emission from the Galactic center is observed in Fermi data. If such observation is finally confirmed it is certainly the first signal from DM particles, as line spectrum is thought the smoking gun of DM annihilation.

The detection of neutrinos is usually difficult. However, as the running of IceCube constraints on DM from neutrino observation are given. In some cases they can be stronger than the direct detection. Especially the sensitivity of direct detection for the SD interaction is weak. In this case the detection of neutrinos by DM annihilation from the sun gives complementary constraints to direct detection.

In the near future we expect the sensitivity of DM detection will be improved greatly. In direct detection the upcoming experiments will improve the present sensitivity by two orders of magnitude. In collider search LHC will upgrade its center of mass energy to 13–14 TeV and improve the probe range of DM mass. The AMS02 is accumulating data right now and will greatly improve the CR spectrum measurement. DAMPE is expected to measure electron spectrum up to 10 TeV precisely. We expect the AMS02 and DAMPE will solve the anomaly in cosmic rays finally.

Acknowledgements We thank Zhaohuan Yu for help in the manuscript preparation. This work was supported by the National Natural Science Foundation of China under the grant Nos. 11075169, 11135009, 11105155, 11105157, and 11175251.

References and notes

1. G. Hinshaw, D. Larson, E. Komatsu, D. Spergel, et al., arXiv: 1212.5226, 2012
2. E. Calabrese, R. A. Hlozek, N. Battaglia, E. S. Battistelli, et al., arXiv: 1302.1841, 2013
3. J. Frieman, M. Turner, and D. Huterer, Ann. Rev. Astron. Astrophys., 2008, 46: 385, arXiv: 0803.0982
4. A. G. Riess, et al. [Supernova Search Team], Astron. J., 1998, 116: 1009, arXiv: astro-ph/9805201
5. S. Perlmutter, et al. [Supernova Cosmology Project], Astrophys. J., 1999, 517: 565, arXiv: astro-ph/9812133
6. B. A. Reid, W. J. Percival, D. J. Eisenstein, L. Verde, et al., Mon. Not. R. Astron. Soc., 2010, 404: 60, arXiv: 0907.1659
7. B. A. Reid, L. Samushia, M. White, W. J. Percival, et al., arXiv: 1203.6641, 2012
8. F. Beutler, C. Blake, M. Colless, D. H. Jones, et al., arXiv: 1204.4725, 2012
9. E. Komatsu, et al. [WMAP Collaboration], Astrophys. J. Suppl., 2011, 192: 18, arXiv: 1001.4538
10. M. Kowalski, et al. [Supernova Cosmology Project], Astrophys. J., 2008, 686: 749, arXiv: 0804.4142
11. V. C. Rubin, W. K. Jr. Ford, and N. Thonnard, Astrophys.

J., 1980, 238: 471
12. F. Zwicky, Helv. Phys. Acta, 1933, 6: 110
13. D. Clowe, M. Bradac, A. H. Gonzalez, M. Markevitch, S. W. Randall, C. Jones, and D. Zaritsky, Astrophys. J., 2006, 648(2): L109, arXiv: astro-ph/0608407
14. G. Bertone, D. Hooper, and J. Silk, Phys. Rep., 2005, 405: 279, arXiv: hep-ph/0404175
15. M. W. Goodman and E. Witten, Phys. Rev. D, 1985, 31(12): 3059
16. G. Jungman, M. Kamionkowski, and K. Griest, Phys. Rep., 1996, 267: 195, arXiv: hep-ph/9506380
17. J. Lewin and P. Smith, Astropart. Phys., 1996, 6: 87
18. V. Zacek, arXiv: 0707.0472, 2007
19. E. Armengaud, arXiv: 1003.2380, 2010
20. L. E. Strigari, arXiv: 1211.7090, 2012
21. R. Bernabei, et al. [DAMA Collaboration], Eur. Phys. J. C, 2008, 56: 333, arXiv: 0804.2741
22. H. Lee, et al. [KIMS Collaboration], Phys. Rev. Lett., 2007, 99: 091301, arXiv: 0704.0423
23. Z. Ahmed, et al. [CDMS-II Collaboration], Science, 2010, 327: 1619, arXiv: 0912.3592
24. C. Aalseth, et al. [CoGeNT Collaboration], Phys. Rev. Lett., 2011, 106: 131301, arXiv: 1002.4703
25. G. Angloher, M. Bauer, I. Bavykina, A. Bento, et al., Eur. Phys. J. C, 2012, 72: 1971, arXiv: 1109.0702
26. E. Armengaud, et al. [EDELWEISS Collaboration], Phys. Lett. B, 2011, 702: 329, arXiv: 1103.4070
27. S. Lin, et al. [TEXONO Collaboration], Phys. Rev. D, 2009, 79: 061101, arXiv: 0712.1645
28. K.-J. Kang, J.-P. Cheng, J. Li, Y.-J. Li, et al., arXiv: 1303.0601, 2013
29. E. Aprile, et al. [XENON100 Collaboration], Phys. Rev. Lett., 2012, 109: 181301, arXiv: 1207.5988
30. D. Y. Akimov, H. Araujo, E. Barnes, V. Belov, et al., Phys. Lett. B, 2012, 709: 14, 1110.4769
31. Z. Li, K. L. Giboni, H. Gong, X. Ji, and A. Tan, arXiv: 1207.5100, 2012
32. E. Behnke, et al. [COUPP Collaboration], Phys. Rev. D, 2012, 86: 052001, arXiv: 1204.3094
33. S. Archambault, et al. [PICASSO Collaboration], Phys. Lett. B, 2012, 711: 153, arXiv: 1202.1240
34. M. Felizardo, T. Girard, T. Morlat, A. Fernandes, et al., Phys. Rev. Lett., 2012, 108: 201302, arXiv: 1106.3014
35. R. Bernabei, et al. [DAMA Collaboration], Phys. Lett. B, 2000, 480: 23
36. C. Savage, G. Gelmini, P. Gondolo, and K. Freese, J. Cosmol. Astropart. Phys., 2009, 0904: 010, arXiv: 0808.3607
37. S. Chang, A. Pierce, and N. Weiner, Phys. Rev. D, 2009, 79: 115011, arXiv: 0808.0196
38. P. Draper, T. Liu, C. E. Wagner, L.-T. Wang, and H. Zhang, Phys. Rev. Lett., 2011, 106: 121805, arXiv: 1009.3963
39. P. Belli, R. Bernabei, A. Bottino, F. Cappella, et al., Phys. Rev. D, 2011, 84: 055014, arXiv: 1106.4667
40. Z. Kang, T. Li, T. Liu, C. Tong, and J. M. Yang, J. Cosmol. Astropart. Phys., 2011, 1101: 028, arXiv: 1008.5243
41. D. E. Kaplan, M. A. Luty, and K. M. Zurek, Phys. Rev. D, 2009, 79: 115016, arXiv: 0901.4117
42. R. Foot, Phys. Rev. D, 2010, 82: 095001, arXiv: 1008.0685
43. C. Aalseth, P. Barbeau, J. Colaresi, J. Collar, et al., Phys. Rev. Lett., 2011, 107: 141301, arXiv: 1106.0650
44. A. L. Fitzpatrick, D. Hooper, and K. M. Zurek, Phys. Rev. D, 2010, 81: 115005, arXiv: 1003.0014
45. S. Chang, J. Liu, A. Pierce, N. Weiner, and I. Yavin, J. Cosmol. Astropart. Phys., 2010, 1008: 018, arXiv: 1004.0697
46. T. Schwetz and J. Zupan, J. Cosmol. Astropart. Phys., 2011, 1108: 008, arXiv: 1106.6241
47. P. J. Fox, J. Kopp, M. Lisanti, and N. Weiner, Phys. Rev. D, 2012, 85: 036008, arXiv: 1107.0717
48. M. Farina, D. Pappadopulo, A. Strumia, and T. Volansky, J. Cosmol. Astropart. Phys., 2011, 1111: 010, arXiv: 1107.0715
49. D. Hooper, J. Collar, J. Hall, D. McKinsey, and C. Kelso, Phys. Rev. D, 2010, 82: 123509, arXiv: 1007.1005
50. C. Arina, Phys. Rev. D, 2012, 86: 123527, arXiv: 1210.4011
51. J. Kopp, T. Schwetz, and J. Zupan, J. Cosmol. Astropart. Phys., 2012, 1203: 001, arXiv: 1110.2721
52. J. Angle, et al. [XENON10 Collaboration], Phys. Rev. Lett., 2011, 107: 051301, arXiv: 1104.3088
53. Z. Ahmed, et al. [CDMS-II Collaboration], Phys. Rev. Lett., 2011, 106: 131302, arXiv: 1011.2482
54. K. Blum, arXiv: 1110.0857, 2011
55. J. Pradler, B. Singh, and I. Yavin, arXiv: 1210.5501, 2012
56. T. Schwetz, PoS IDM, 2011, 2010: 070, arXiv: 1011.5432
57. P. J. Fox, J. Liu, and N.Weiner, Phys. Rev. D, 2011, 83: 103514, arXiv: 1011.1915
58. J. L. Feng, J. Kumar, D. Marfatia, and D. Sanford, Phys. Lett. B, 2011, 703: 124, arXiv: 1102.4331
59. X. Gao, Z. Kang, and T. Li, arXiv: 1107.3529, 2011
60. S. Chang, A. Pierce, and N. Weiner, J. Cosmol. Astropart. Phys., 2010, 1001: 006, arXiv: 0908.3192
61. H. An, S.-L. Chen, R. N. Mohapatra, S. Nussinov, and Y. Zhang, Phys. Rev. D, 2010, 82: 023533, arXiv: 1004.3296
62. D. Tucker-Smith and N. Weiner, Phys. Rev. D, 2001, 64: 043502, arXiv: hep-ph/0101138
63. S. Chang, G. D. Kribs, D. Tucker-Smith, and N.Weiner, Phys. Rev. D, 2009, 79: 043513, arXiv: 0807.2250
64. J. M. Cline, Z. Liu, and W. Xue, arXiv: 1207.3039, 2012
65. S.-L. Chen and Y. Zhang, Phys. Rev. D, 2011, 84: 031301, arXiv: 1106.4044
66. J. Kumar, D. Sanford, and L. E. Strigari, Phys. Rev. D, 2012, 85: 081301, arXiv: 1112.4849
67. H.-B. Jin, S. Miao, and Y.-F. Zhou, arXiv: 1207.4408, 2012
68. E. Aprile, et al. [XENON100 Collaboration], Phys. Rev. D, 2011, 84: 061101, arXiv: 1104.3121

69. C. Strege, G. Bertone, D. Cerdeno, M. Fornasa, et al., J. Cosmol. Astropart. Phys., 2012, 1203: 030, arXiv: 1112.4192
70. A. Fowlie, M. Kazana, K. Kowalska, S. Munir, et al., Phys. Rev. D, 2012, 86: 075010, arXiv: 1206.0264
71. O. Buchmueller, R. Cavanaugh, A. De Roeck, M. Dolan, et al., Eur. Phys. J. C, 2012, 72: 2020, arXiv: 1112.3564
72. E. Aprile [XENON1T Collaboration], arXiv: 1206.6288, 2012
73. T. Aaltonen, et al. [CDF Collaboration], Phys. Rev. Lett., 2012, 108: 211804, arXiv: 1203.0742
74. G. Aad, et al. [ATLAS Collaboration], arXiv: 1210.4491, 2012
75. P. de Jong [ATLAS and CMS Collaborations], arXiv: 1211.3887, 2012
76. A. Djouadi, J. Lykken, K. Mönig, Y. Okada, et al., arXiv: 0709.1893, 2007
77. H.-C. Cheng, J. F. Gunion, Z. Han, G. Marandella, and B. McElrath, J. High Energy Phys., 2007, 0712: 076, arXiv: 0707.0030
78. M. Burns, K. Kong, K. T. Matchev, and M. Park, J. High Energy Phys., 2009, 0903: 143, arXiv: 0810.5576
79. A. J. Barr and C. G. Lester, J. Phys. G, 2010, 37: 123001, arXiv: 1004.2732
80. T. Han, I.-W. Kim, and J. Song, arXiv: 1206.5633, 2012
81. H. Baer and X. Tata, arXiv: 0805.1905, 2008
82. H. Baer, arXiv: 0901.4732, 2009
83. Y. Bai and T. M. Tait, arXiv: 1208.4361, 2012
84. L. M. Carpenter, A. Nelson, C. Shimmin, T. M. Tait, and D. Whiteson, arXiv: 1212.3352, 2012
85. Y. Bai, P. J. Fox, and R. Harnik, J. High Energy Phys., 2010,1012: 048, arXiv: 1005.3797
86. J. Goodman, M. Ibe, A. Rajaraman, W. Shepherd, et al., Phys. Rev. D, 2010, 82: 116010, arXiv: 1008.1783
87. J. L. Feng, S. Su, and F. Takayama, Phys. Rev. Lett., 2006, 96(15): 151802, arXiv: hep-ph/0503117
88. P. J. Fox, R. Harnik, J. Kopp, and Y. Tsai, Phys. Rev. D, 2012, 85: 056011, arXiv: 1109.4398
89. A. Birkedal, K. Matchev, and M. Perelstein, Phys. Rev. D, 2004, 70(7): 077701, arXiv: hep-ph/0403004
90. P. J. Fox, R. Harnik, J. Kopp, and Y. Tsai, Phys. Rev. D, 2011, 84: 014028, arXiv: 1103.0240
91. H. Dreiner, M. Huck, M. Kramer, D. Schmeier, and J. Tattersall, arXiv: 1211.2254, 2012
92. M. Beltran, D. Hooper, E.W. Kolb, and Z. C. Krusberg, Phys. Rev. D, 2009, 80: 043509, arXiv: 0808.3384
93. Q.-H. Cao, C.-R. Chen, C. S. Li, and H. Zhang, J. High Energy Phys., 2011, 1108: 018, arXiv: 0912.4511
94. J.-M. Zheng, Z.-H. Yu, J.-W. Shao, X.-J. Bi, et al., Nucl. Phys. B, 2012, 854: 350, arXiv: 1012.2022
95. Z.-H. Yu, J.-M. Zheng, X.-J. Bi, Z. Li, et al., Nucl. Phys. B, 2012, 860: 115, arXiv: 1112.6052
96. S. Chatrchyan, et al. [CMS Collaboration], J. High Energy Phys., 2012, 1209: 094, arXiv: 1206.5663
97. M. Ackermann, et al. [Fermi-LAT Collaboration], Phys. Rev. Lett., 2011, 107: 241302, arXiv: 1108.3546
98. J. Goodman and W. Shepherd, arXiv: 1111.2359, 2011
99. H. Baer, X. Tata, and J. Woodside, Phys. Rev. D, 1992, 45(1): 142
100. D. Feldman, Z. Liu, and P. Nath, J. High Energy Phys., 2008, 0804: 054, arXiv: 0802.4085
101. S. Chatrchyan, et al. [CMS Collaboration], Phys. Rev. Lett., 2012, 109: 171803, arXiv: 1207.1898
102. G. Aad, et al. [ATLAS Collaboration], arXiv: 1208.0949, 2012
103. C. Rogan, arXiv: 1006.2727, 2010
104. CMS Collaboration, CMS-PAS-SUS-12-005, 2012, http://cdsweb.cern.ch/record/1430715
105. L. Randall and D. Tucker-Smith, Phys. Rev. Lett., 2008, 101: 221803, arXiv: 0806.1049
106. S. Chatrchyan, et al. [CMS Collaboration], arXiv: 1210.8115, 2012
107. C. Lester and D. Summers, Phys. Lett. B, 1999, 463(1): 99, arXiv: hep-ph/9906349
108. A. Barr, C. Lester, and P. Stephens, J. Phys. G, 2003, 29: 2343, arXiv: hep-ph/0304226
109. S. Chatrchyan, et al. [CMS Collaboration], J. High Energy Phys., 2012, 1210: 018, arXiv: 1207.1798
110. S. Chatrchyan, et al. [CMS Collaboration], J. High Energy Phys., 2011, 1108: 155, arXiv: 1106.4503
111. ALEPH, DELPHI, L3 and OPAL Collaborations, Joint SUSY Working Group, 2002, LEPSUSYWG/02-06-2
112. R. Kitano and Y. Nomura, Phys. Rev. D, 2006, 73(9): 095004, arXiv: hep-ph/0602096
113. M. Papucci, J. T. Ruderman, and A. Weiler, J. High Energy Phys., 2012, 1209: 035, arXiv: 1110.6926
114. Z. Kang, J. Li, and T. Li, J. High Energy Phys., 2012, 1211: 024, arXiv: 1201.5305
115. J.-J. Cao, Z.-X. Heng, J. M. Yang, Y.-M. Zhang, and J.-Y. Zhu, J. High Energy Phys., 2012, 1203: 086, arXiv: 1202.5821
116. G. Aad, et al. [ATLAS Collaboration], Eur. Phys. J. C, 2012, 72: 2174, arXiv: 1207.4686
117. ATLAS Collaboration, ATLAS-CONF-2012-103, 2012, http://cds.cern.ch/record/1472672
118. X.-J. Bi, Q.-S. Yan, and P.-F. Yin, Phys. Rev. D, 2012, 85: 035005, arXiv: 1111.2250
119. J. Cao, C. Han, L. Wu, J. M. Yang, and Y. Zhang, J. High Energy Phys., 2012, 1211: 039, arXiv: 1206.3865
120. G. Aad, et al. [ATLAS Collaboration], arXiv: 1208.2590, 2012
121. G. Aad, et al. [ATLAS Collaboration], arXiv: 1208.1447, 2012
122. M. Carena, A. Freitas, and C. Wagner, J. High Energy Phys., 2008, 0810: 109, arXiv: 0808.2298

123. M. A. Ajaib, T. Li, and Q. Shafi, Phys. Rev. D, 2012, 85: 055021, arXiv: 1111.4467
124. Z.-H. Yu, X.-J. Bi, Q.-S. Yan, and P.-F. Yin, arXiv: 1211.2997, 2012
125. S. Chatrchyan, et al. [CMS Collaboration], J. High Energy Phys., 2012, 1211: 147, arXiv: 1209.6620
126. G. Aad, et al. [ATLAS Collaboration], arXiv: 1208.3144, 2012
127. A. Arvanitaki, S. Dimopoulos, A. Pierce, S. Rajendran, and J. G. Wacker, Phys. Rev. D, 2007, 76(5): 055007, arXiv: hep-ph/0506242
128. M. Johansen, J. Edsjo, S. Hellman, and D. Milstead, J. High Energy Phys., 2010, 1008: 005, arXiv: 1003.4540
129. G. Giudice and R. Rattazzi, Phys. Rep., 1999, 322: 419, arXiv: hep-ph/9801271
130. S. Dimopoulos, M. Dine, S. Raby, and S. D. Thomas, Phys. Rev. Lett., 1996, 76(19): 3494, arXiv: hep-ph/9601367
131. S. Chatrchyan, et al. [CMS Collaboration], arXiv: 1212.1838, 2012
132. G. Aad, et al. [ATLAS Collaboration], arXiv: 1211.1597, 2012
133. S. Chatrchyan, et al. [CMS Collaboration], Phys. Lett. B, 2012, 713: 408, arXiv: 1205.0272
134. O. Adriani, et al. [PAMELA Collaboration], Nature, 2009, 458: 607, arXiv: 0810.4995
135. A. Strong and I. Moskalenko, Astrophys. J., 1998, 509(1): 212, arXiv: astro-ph/9807150, available at: http://galprop.stanford.edu/
136. L. Gleeson and W. Axford, Astrophys. J., 1968, 154: 1011
137. S. Barwick, et al. [HEAT Collaboration], Astrophys. J., 1997, 482: L191, arXiv: astro-ph/9703192
138. M. Aguilar, et al. [AMS-01 Collaboration], Phys. Lett. B, 2007, 646: 145, arXiv: astro-ph/0703154
139. R. Golden, S. J. Stochaj, S. A. Stephens, F. Aversa, et al., Astrophys. J., 1996, 457(2): L103
140. M. Boezio, P. Carlson, T. Francke, N. Weber, et al., Astrophys. J., 2000, 532(1): 653
141. S. Coutu, A. Beach, J. Beatty, A. Bhattacharyya, et al., International Cosmic Ray Conference, 2011, 5: 1687
142. M. Ackermann, et al. [Fermi-LAT Collaboration], Phys. Rev. Lett., 2012, 108: 011103, arXiv: 1109.0521
143. J. Mitchell, L. Barbier, E. Christian, J. Krizmanic, K. Krombel, J. Ormes, R. Streitmatter, A. Labrador, A. Davis, R. Mewaldt, S. Schindler, R. Golden, S. Stochaj, W. Webber, W. Menn, M. Hof, O. Reimer, M. Simon, and I. Rasmussen, Phys. Rev. Lett., 1996, 76(17): 3057
144. A. Beach, J. Beatty, A. Bhattacharyya, C. Bower, S. Coutu, M. DuVernois, A. Labrador, S. McKee, S. Minnick, D. Müller, J. Musser, S. Nutter, M. Schubnell, S. Swordy, G. Tarlé, and A. Tomasch, Phys. Rev. Lett., 2001, 87(27): 271101, arXiv: astro-ph/0111094
145. M. Boezio, P. Carlson, T. Francke, N. Weber, et al., Astrophys. J., 1997, 487(1): 415
146. M. Boezio, et al. [WiZard/CAPRICE Collaboration], Astrophys. J., 2001, 561: 787, arXiv: astro-ph/0103513
147. S. Orito, et al. [BESS Collaboration], Phys. Rev. Lett., 2000, 84: 1078, arXiv: astro-ph/9906426
148. Y. Asaoka, Y. Shikaze, K. Abe, K. Anraku, et al., Phys. Rev. Lett., 2002, 88(5): 051101, arXiv: astro-ph/0109007
149. K. Abe, H. Fuke, S. Haino, T. Hams, et al., Phys. Lett. B, 2008, 670: 103, arXiv: 0805.1754
150. O. Adriani, G. Barbarino, G. Bazilevskaya, R. Bellotti, et al., Phys. Rev. Lett., 2009, 102: 051101, arXiv: 0810.4994
151. J. Alcaraz, et al. [AMS Collaboration], Phys. Lett. B, 2000, 484: 10
152. S. Barwick, J. Beatty, C. Bower, C. Chaput, S. Coutu, G. A. de Nolfo, M. A. DuVernois, D. Ellithorpe, D. Ficenec, J. Knapp, D. M. Lowder, S. McKee, D. Muller, J. A. Musser, S. L. Nutter, E. Schneider, S. P. Swordy, G. Tarle, A. D. Tomasch, and E. Torbet, Astrophys. J., 1998, 498(2): 779, arXiv: astro-ph/9712324
153. T. Kobayashi, J. Nishimura, Y. Komori, T. Shirai, et al., International Cosmic Ray Conference, 1999, 3: 61
154. O. Adriani, et al. [PAMELA Collaboration], Phys. Rev. Lett., 2011, 106: 201101, arXiv: 1103.2880
155. J. Chang, J. Adams, H. Ahn, G. Bashindzhagyan, M. Christl, O. Ganel, T. G. Guzik, J. Isbert, K. C. Kim, E. N. Kuznetsov, M. I. Panasyuk, A. D. Panov, W. K. H. Schmidt, E. S. Seo, N. V. Sokolskaya, J. W. Watts, J. P. Wefel, J. Wu, and V. I. Zatsepin, Nature, 2008, 456(7220): 362
156. F. Aharonian, et al. [HESS Collaboration], Phys. Rev. Lett., 2008, 101: 261104, arXiv: 0811.3894
157. F. Aharonian, et al. [HESS Collaboration], Astron. Astrophys., 2009, 508: 561, arXiv: 0905.0105
158. A. A. Abdo, et al. [Fermi-LAT Collaboration], Phys. Rev. Lett., 2009, 102: 181101, arXiv: 0905.0025
159. D. Grasso, et al. [FERMI-LAT Collaboration], Astropart. Phys., 2009, 32: 140, arXiv: 0905.0636
160. Y.-Z. Fan, B. Zhang, and J. Chang, Int. J. Mod. Phys. D, 2011, 19: 2011, arXiv: 1008.4646
161. T. Delahaye, F. Donato, N. Fornengo, J. Lavalle, et al., Astron. Astrophys., 2009, 501: 821, arXiv: 0809.5268
162. P. D. Serpico, Phys. Rev. D, 2009, 79: 021302, arXiv: 0810.4846
163. P. D. Serpico, Astropart. Phys., 2012, 39-40: 2, arXiv: 1108.4827
164. K. Auchettl and C. Balazs, Astrophys. J., 2012, 749: 184, arXiv: 1106.4138
165. N. J. Shaviv, E. Nakar, and T. Piran, Phys. Rev. Lett., 2009, 103: 111302, arXiv: 0902.0376
166. J. Stockton, Astropart. Phys., 2011, 35: 161, arXiv: 1107.1696
167. L. Stawarz, V. Petrosian, and R. D. Blandford, Astrophys. J., 2010, 710: 236, arXiv: 0908.1094
168. H. Yuksel, M. D. Kistler, and T. Stanev, Phys. Rev. Lett., 2009, 103: 051101, arXiv: 0810.2784

169. D. Hooper, P. Blasi, and P. D. Serpico, J. Cosmol. Astropart. Phys., 2009, 0901: 025, arXiv: 0810.1527
170. S. Profumo, Central Eur. J. Phys., 2011, 10: 1, arXiv: 0812.4457
171. D. Malyshev, I. Cholis, and J. Gelfand, Phys. Rev. D, 2009, 80: 063005, arXiv: 0903.1310
172. N. Kawanaka, K. Ioka, and M. M. Nojiri, Astrophys. J., 2010, 710: 958, arXiv: 0903.3782
173. J. S. Heyl, R. Gill, and L. Hernquist, Mon. Not. R. Astron. Soc., 2010, 406: L25, arXiv: 1005.1003
174. J. Arons, IAU Symposium, 1981, 94: 175
175. A. K. Harding and R. Ramary, International Cosmic Ray Conference, 1987, 2: 92
176. L. Zhang and K. Cheng, Astron. Astrophys., 2001, 368(3): 1063
177. C. Grimani, Astron. Astrophys., 2007, 474(2): 339
178. E. Aliu, et al. [VERITAS Collaboration], Science, 2011, 334: 69, arXiv: 1108.3797
179. J. Aleksic, et al. [MAGIC Collaboration], Astrophys. J., 2011, 742: 43, arXiv: 1108.5391
180. I. Cernuda, Astropart. Phys., 2010, 34: 59, arXiv: 0905.1653
181. P. Blasi, Phys. Rev. Lett., 2009, 103: 051104, arXiv: 0903.2794
182. Y. Fujita, K. Kohri, R. Yamazaki, K. Ioka, et al., Phys. Rev. D, 2009, 80: 063003, arXiv: 0903.5298
183. M. Ahlers, P. Mertsch, and S. Sarkar, Phys. Rev. D, 2009, 80: 123017, arXiv: 0909.4060
184. H. B. Hu, Q. Yuan, B. Wang, C. Fan, J. L. Zhang, and X. J. Bi, Astrophys. J., 2009, 700(2): L170
185. P. Biermann, J. Becker, A. Meli, W. Rhode, et al., Phys. Rev. Lett., 2009, 103: 061101, arXiv: 0903.4048
186. K. Ioka, Prog. Theor. Phys., 2010, 123: 743, arXiv: 0812.4851
187. K. Kashiyama, K. Ioka, and N. Kawanaka, Phys. Rev. D, 2011, 83: 023002, arXiv: 1009.1141
188. T. Kamae, S.-H. Lee, L. Baldini, F. Giordano, M.-H. Grondin, L. Latronico, M. Lemoine-Goumard, C. Sgró, T. Tanaka, and Y. Uchiyama, arXiv: 1010.3477, 2010
189. P. Blasi and P. D. Serpico, Phys. Rev. Lett., 2009, 103: 081103, arXiv: 0904.0871
190. P. Mertsch and S. Sarkar, Phys. Rev. Lett., 2009, 103: 081104, arXiv: 0905.3152
191. P.-F. Yin, Q. Yuan, J. Liu, J. Zhang, X.-J. Bi, S.-H. Zhu, and X. M. Zhang, Phys. Rev. D, 2009, 79: 023512, arXiv: 0811.0176
192. L. Bergstrom, T. Bringmann, and J. Edsjo, Phys. Rev. D, 2008, 78: 103520, arXiv: 0808.3725
193. V. Barger, W. Y. Keung, D. Marfatia, and G. Shaughnessy, Phys. Lett. B, 2009, 672: 141, arXiv: 0809.0162
194. M. Cirelli, M. Kadastik, M. Raidal, and A. Strumia, Nucl. Phys. B, 2009, 813: 1, arXiv: 0809.2409
195. F. Donato, D. Maurin, P. Brun, T. Delahaye, and P. Salati, Phys. Rev. Lett., 2009, 102: 071301, arXiv: 0810.5292
196. J. Lavalle, Q. Yuan, D. Maurin, and X. Bi, Astron. Astrophys., 2008, 479: 427, arXiv: 0709.3634
197. Q. Yuan, X.-J. Bi, J. Liu, P.-F. Yin, J. Zhang, and S.-H. Zhu, J. Cosmol. Astropart. Phys., 2009, 0912: 011, arXiv: 0905.2736
198. D. Hooper, A. Stebbins, and K. M. Zurek, Phys. Rev. D, 2009, 79: 103513, arXiv: 0812.3202
199. P. Brun, T. Delahaye, J. Diemand, S. Profumo, and P. Salati, Phys. Rev. D, 2009, 80: 035023, arXiv: 0904.0812
200. R. Jeannerot, X. Zhang, and R. H. Brandenberger, J. High Energy Phys., 1999, 9912: 003, arXiv: hep-ph/9901357
201. W. Lin, D. Huang, X. Zhang, and R. H. Brandenberger, Phys. Rev. Lett., 2001, 86(6): 954, arXiv: astro-ph/0009003
202. X.-J. Bi, R. Brandenberger, P. Gondolo, T.-J. Li, Q. Yuan, and X. M. Zhang, Phys. Rev. D, 2009, 80: 103502, arXiv: 0905.1253
203. Q. Yuan, Y. Cao, J. Liu, P.-F. Yin, L.Gao, X.-J. Bi, and X. M. Zhang, Phys. Rev. D, 2012, 86: 103531, arXiv: 1203.5636
204. K. Griest and D. Seckel, Phys. Rev. D, 1991, 43(10): 3191
205. P. Gondolo and G. Gelmini, Nucl. Phys. B, 1991, 360(1): 145
206. D. Feldman, Z. Liu, and P. Nath, Phys. Rev. D, 2009, 79: 063509, arXiv: 0810.5762
207. M. Ibe, H. Murayama, and T. Yanagida, Phys. Rev. D, 2009, 79: 095009, arXiv: 0812.0072
208. W.-L. Guo and Y.-L. Wu, Phys. Rev. D, 2009, 79: 055012, arXiv: 0901.1450
209. X.-J. Bi, X.-G. He, and Q. Yuan, Phys. Lett. B, 2009, 678: 168, arXiv: 0903.0122
210. X.-J. Bi, P.-F. Yin, and Q. Yuan, Phys. Rev. D, 2012, 85: 043526, arXiv: 1106.6027
211. M. Pospelov and A. Ritz, Phys. Lett. B, 2009, 671: 391, arXiv: 0810.1502
212. N. Arkani-Hamed, D. P. Finkbeiner, T. R. Slatyer, and N. Weiner, Phys. Rev. D, 2009, 79: 015014, arXiv: 0810.0713
213. M. Lattanzi and J. I. Silk, Phys. Rev. D, 2009, 79: 083523, arXiv: 0812.0360
214. J. Hisano, S. Matsumoto, M. M. Nojiri, and O. Saito, Phys. Rev. D, 2005, 71(6): 063528, arXiv: hep-ph/0412403
215. I. Cholis, D. P. Finkbeiner, L. Goodenough, and N. Weiner, J. Cosmol. Astropart. Phys., 2009, 0912: 007, arXiv: 0810.5344
216. Y. Nomura and J. Thaler, Phys. Rev. D, 2009, 79: 075008, arXiv: 0810.5397
217. J. Zavala, M. Vogelsberger, and S. D. White, Phys. Rev. D, 2010, 81: 083502, arXiv: 0910.5221
218. J. B. Dent, S. Dutta, and R. J. Scherrer, Phys. Lett. B, 2010, 687: 275, arXiv: 0909.4128
219. J. L. Feng, M. Kaplinghat, and H.-B. Yu, Phys. Rev. D, 2010, 82: 083525, arXiv: 1005.4678

220. J. L. Feng, M. Kaplinghat, and H.-B. Yu, Phys. Rev. Lett., 2010, 104: 151301, arXiv: 0911.0422

221. T. R. Slatyer, N. Toro, and N. Weiner, Phys. Rev. D, 2012, 86: 083534, arXiv: 1107.3546

222. M. Baumgart, C. Cheung, J. T. Ruderman, L.-T.Wang, and I. Yavin, J. High Energy Phys., 2009, 0904: 014, arXiv: 0901.0283

223. C. Cheung, J. T. Ruderman, L.-T. Wang, and I. Yavin, Phys. Rev. D, 2009, 80: 035008, arXiv: 0902.3246

224. M. Reece and L.-T. Wang, J. High Energy Phys., 2009, 0907: 051, arXiv: 0904.1743

225. J. D. Bjorken, R. Essig, P. Schuster, and N. Toro, Phys. Rev. D, 2009, 80: 075018, arXiv: 0906.0580

226. M. Freytsis, G. Ovanesyan, and J. Thaler, J. High Energy Phys., 2010, 1001:111, arXiv: 0909.2862

227. R. Essig, P. Schuster, and N. Toro, Phys. Rev. D, 2009, 80: 015003, arXiv: 0903.3941

228. P.-F. Yin, J. Liu, and S.-H. Zhu, Phys. Lett. B, 2009, 679: 362, arXiv: 0904.4644

229. H.-B. Li and T. Luo, Phys. Lett. B, 2010, 686: 249, arXiv: 0911.2067

230. Y. Bai and Z. Han, Phys. Rev. Lett., 2009, 103: 051801, arXiv: 0902.0006

231. C. Cheung, J. T. Ruderman, L.-T. Wang, and I. Yavin, J. High Energy Phys., 2010, 1004: 116, arXiv: 0909.0290

232. C.-R. Chen and F. Takahashi, J. Cosmol. Astropart. Phys., 2009, 0902: 004, arXiv: 0810.4110

233. K. Ishiwata, S. Matsumoto, and T. Moroi, Phys. Lett. B, 2009, 675: 446, arXiv: 0811.0250

234. A. Ibarra and D. Tran, J. Cosmol. Astropart. Phys., 2009, 0902: 021, arXiv: 0811.1555

235. C.-R. Chen, M. M. Nojiri, F. Takahashi, and T. Yanagida, Prog. Theor. Phys., 2009, 122: 553, arXiv: 0811.3357

236. E. Nardi, F. Sannino, and A. Strumia, J. Cosmol. Astropart. Phys., 2009, 0901: 043, arXiv: 0811.4153

237. A. Arvanitaki, S. Dimopoulos, S. Dubovsky, P. W. Graham, R. Harnik, and S. Rajendran, Phys. Rev. D, 2009, 79: 105022, arXiv: 0812.2075

238. P. Meade, M. Papucci, A. Strumia, and T. Volansky, Nucl. Phys. B, 2010, 831: 178, arXiv: 0905.0480

239. M. Papucci and A. Strumia, J. Cosmol. Astropart. Phys., 2010, 1003: 014, arXiv: 0912.0742

240. C.-R. Chen, S. K. Mandal, and F. Takahashi, J. Cosmol. Astropart. Phys., 2010, 1001: 023, arXiv: 0910.2639

241. A. Ibarra, D. Tran, and C. Weniger, Phys. Rev. D, 2010, 81: 023529, arXiv: 0909.3514

242. L. Zhang, C. Weniger, L. Maccione, J. Redondo, and G. Sigl, J. Cosmol. Astropart. Phys., 2010, 1006: 027, arXiv: 0912.4504

243. X. Huang, G. Vertongen, and C. Weniger, J. Cosmol. Astropart. Phys., 2012, 1201: 042, arXiv: 1110.1529

244. M. Cirelli, E. Moulin, P. Panci, P. D. Serpico, and A. Viana, Phys. Rev. D, 2012, 86: 083506, arXiv: 1205.5283

245. J. Hisano, M. Kawasaki, K. Kohri, and K. Nakayama, Phys. Rev. D, 2009, 79: 043516, arXiv: 0812.0219

246. L. Covi, M. Grefe, A. Ibarra, and D. Tran, J. Cosmol. Astropart. Phys., 2010, 1004: 017, arXiv: 0912.3521

247. J. Liu, Q. Yuan, X. Bi, H. Li, and X. Zhang, Phys. Rev. D, 2010, 81: 023516, arXiv: 0906.3858

248. J. Liu, Q. Yuan, X.-J. Bi, H. Li, and X. Zhang, Phys. Rev. D, 2012, 85: 043507, arXiv: 1106.3882

249. J. Hall and D. Hooper, Phys. Lett. B, 2009, 681: 220, arXiv: 0811.3362

250. AMS-02, http://www.ams02.org/

251. M. Pato, M. Lattanzi, and G. Bertone, J. Cosmol. Astropart. Phys., 2010, 1012: 020, arXiv: 1010.5236

252. F. Palmonari, V. Bindi, A. Contin, N. Masi, and L. Quadrani [AMS-02 Collaboration], J. Phys. Conf. Ser., 2011, 335: 012066

253. J. Chang, in: The 7th International Workshop "Dark Side of the Universe (DSU 2011)", 2011

254. E. Borriello, A. Cuoco, and G. Miele, Astrophys. J., 2009, 699: L59, arXiv: 0903.1852

255. V. Barger, Y. Gao, W. Y. Keung, D. Marfatia, and G. Shaughnessy, Phys. Lett. B, 2009, 678: 283, arXiv: 0904.2001

256. M. Cirelli and P. Panci, Nucl. Phys. B, 2009, 821: 399, arXiv: 0904.3830

257. M. Regis and P. Ullio, Phys. Rev. D, 2009, 80: 043525, arXiv: 0904.4645

258. S. Matsumoto, K. Ishiwata, and T. Moroi, Phys. Lett. B, 2009, 679: 1, arXiv: 0905.4593

259. L. Zhang, J. Redondo, and G. Sigl, J. Cosmol. Astropart. Phys., 2009, 0909: 012, arXiv: 0905.4952

260. A. Ibarra, D. Tran, and C. Weniger, J. Cosmol. Astropart. Phys., 2010, 1001: 009, arXiv: 0906.1571

261. I. Cholis, G. Dobler, D. P. Finkbeiner, L. Goodenough, T. R. Slatyer, and N. Weiner, arXiv: 0907.3953, 2009

262. J. Zhang, Q. Yuan, and X.-J. Bi, Astrophys. J., 2010, 720: 9, arXiv: 0908.1236

263. X.-J. Bi, X.-G. He, E. Ma, and J. Zhang, Phys. Rev. D, 2010, 81: 063522, arXiv: 0910.0771

264. J. P. Harding and K. N. Abazajian, Phys. Rev. D, 2010, 81: 023505, arXiv: 0910.4590

265. M. Pohl and D. Eichler, arXiv: 0912.1203, 2009

266. Q. Yuan, B. Yue, X.-J. Bi, X. Chen, and X. Zhang, J. Cosmol. Astropart. Phys., 2010,1010: 023, arXiv: 0912.2504

267. Q. Yuan, P.-F. Yin, X.-J. Bi, X.-M. Zhang, and S.-H. Zhu, Phys. Rev. D, 2010, 82: 023506, arXiv: 1002.0197

268. J. Zhang, X.-J. Bi, J. Liu, S.-M. Liu, P.-F. Yin, Q. Yuan, and S.-H. Zhu, Phys. Rev. D, 2009, 80: 023007, arXiv: 0812.0522

269. S. Hunter, D. Bertsch, J. Catelli, T. Digel, et al., Astrophys. J., 1997, 481(1): 205

270. J. Einasto, Trudy Astrofizicheskogo Instituta Alma-Ata, 1965, 5: 87
271. J. Wolf, G. D. Martinez, J. S. Bullock, M. Kaplinghat, et al., Mon. Not. R. Astron. Soc., 2010, 406: 1220, arXiv: 0908.2995
272. A. Abdo, et al. [Fermi-LAT Collaboration], Astrophys. J., 2010, 712: 147, arXiv: 1001.4531
273. A. Geringer-Sameth and S. M. Koushiappas, Phys. Rev. Lett., 2011, 107: 241303, arXiv: 1108.2914
274. I. Cholis and P. Salucci, Phys. Rev. D, 2012, 86: 023528, arXiv: 1203.2954
275. A. Baushev, S. Federici, and M. Pohl, Phys. Rev. D, 2012, 86: 063521, arXiv: 1205.3620
276. M. Mazziotta, F. Loparco, F. de Palma, and N. Giglietto arXiv: 1203.6731, 2012
277. Y.-L. S. Tsai, Q. Yuan, and X. Huang, arXiv: 1212.3990, 2012
278. A. Drlica-Wagner, 4th Fermi Symposium, 2012
279. G. Corcella, I. Knowles, G. Marchesini, S. Moretti, et al., J. High Energy Phys., 2001, 0101: 010, arXiv: hep-ph/0011363
280. T. Sjostrand, S. Mrenna, and P. Z. Skands, J. High Energy Phys., 2006, 0605: 026, arXiv: hep-ph/0603175
281. T. Sjostrand, S. Mrenna, and P. Z. Skands, Comput. Phys. Commun., 2008, 178: 852, arXiv: 0710.3820
282. L. Gao, C. Frenk, A. Jenkins, V. Springel, and S. White, Mon. Not. R. Astron. Soc., 2012, 419: 1721, arXiv: 1107.1916
283. A. Charbonnier, C. Combet, M. Daniel, S. Funk, et al., Mon. Not. R. Astron. Soc., 2011, 418: 1526, arXiv: 1104.0412
284. M. Ackermann, et al. [Fermi-LAT Collaboration], arXiv: 1006.0748, 2010
285. M. Ackermann, M. Ajello, A. Allafort, L. Baldini, J. Ballet, et al., J. Cosmol. Astropart. Phys., 2010, 1005: 025, arXiv: 1002.2239
286. L. Dugger, T. E. Jeltema, and S. Profumo, J. Cosmol. Astropart. Phys., 2010, 1012: 015, arXiv: 1009.5988
287. J. Ke, M. Luo, L. Wang, and G. Zhu, Phys. Lett. B, 2011, 698: 44, arXiv: 1101.5878
288. S. Zimmer, J. Conrad, and A. Pinzke [Fermi-LAT Collaboration], arXiv: 1110.6863, 2011
289. S. Ando and D. Nagai, J. Cosmol. Astropart. Phys., 2012, 1207: 017, arXiv: 1201.0753
290. C. Combet, D. Maurin, E. Nezri, E. Pointecouteau, et al., Phys. Rev. D, 2012, 85: 063517, arXiv: 1203.1164.
291. E. Nezri, R. White, C. Combet, D. Maurin, et al., Mon. Not. R. Astron. Soc., 2012, 425: 477, arXiv: 1203.1165
292. J. Han, C. S. Frenk, V. R. Eke, L. Gao, et al., arXiv: 1207.6749, 2012
293. J. Han, C. S. Frenk, V. R. Eke, L. Gao, and S. D.White, arXiv: 1201.1003, 2012
294. O. Macias-Ramirez, C. Gordon, A. M. Brown, and J. Adams, Phys. Rev. D, 2012, 86: 076004, arXiv: 1207.6257
295. H. Baumgardt, P. Cote, M. Hilker, M. Rejkuba, et al., arXiv: 0904.3329, 2009
296. R. R. Lane, L. L. Kiss, G. F. Lewis, R. A. Ibata, et al., Mon. Not. R. Astron. Soc., 2010, 406: 2732, arXiv: 1004.4696
297. C. Conroy, A. Loeb, and D. Spergel, Astrophys. J., 2011, 741: 72, arXiv: 1010.5783
298. P. J. E. Peebles, Astrophys. J., 1984, 277: 470
299. L. Feng, Q. Yuan, P.-F. Yin, X.-J. Bi, and M. Li, J. Cosmol. Astropart. Phys., 2012, 1204: 030, arXiv: 1112.2438
300. A. A. Abdo, et al. [Fermi-LAT Collaboration], arXiv: 1003.3588, 2010
301. D. Hooper and T. Linden, Phys. Rev. D, 2011, 84: 123005, arXiv: 1110.0006
302. L. Goodenough and D. Hooper, arXiv: 0910.2998, 2009
303. D. Hooper and L. Goodenough, Phys. Lett. B, 2011, 697: 412, arXiv: 1010.2752
304. A. Boyarsky, D. Malyshev, and O. Ruchayskiy, Phys. Lett. B, 2011, 705: 165, arXiv: 1012.5839
305. K. N. Abazajian and M. Kaplinghat, Phys. Rev. D, 2012, 86: 083511, arXiv: 1207.6047
306. J. F. Navarro, C. S. Frenk, and S. D. White, Astrophys. J., 1997, 490(2): 493, arXiv: astro-ph/9611107
307. R. Bernabei, et al. [DAMA Collaboration and LIBRA Collaboration], Eur. Phys. J. C, 2010, 67: 39, arXiv: 1002.1028
308. K. N. Abazajian, J. Cosmol. Astropart. Phys., 2011, 1103: 010, arXiv: 1011.4275
309. N. Bernal and S. Palomares-Ruiz, Nucl. Phys. B, 2012, 857: 380, arXiv: 1006.0477
310. J. Ellis, K. A. Olive, and V. C. Spanos, J. Cosmol. Astropart. Phys., 2011, 1110: 024, arXiv: 1106.0768
311. X. Huang, Q. Yuan, P.-F. Yin, X.-J. Bi, and X. Chen, J. Cosmol. Astropart. Phys., 2012, 1211: 048, arXiv: 1208.0267
312. D. Hooper, C. Kelso, and F. S. Queiroz, arXiv: 1209.3015, 2012
313. M. Cirelli, P. Panci, and P. D. Serpico, Nucl. Phys. B, 2010, 840: 284, arXiv: 0912.0663
314. G. Zaharijas, A. Cuoco, Z. Yang, and J. Conrad [Fermi-LAT Collaboration], PoS IDM, 2011, 2010: 111, arXiv: 1012.0588
315. E. J. Baxter and S. Dodelson, Phys. Rev. D, 2011, 83: 123516, arXiv: 1103.5779
316. M. Ackermann, et al. [Fermi-LAT Collaboration], Phys. Rev. D, 2012, 86: 022002, arXiv: 1205.2739
317. M. Ackermann, et al. [Fermi-LAT Collaboration], Astrophys. J., 2012, 761: 91, arXiv: 1205.6474
318. P. D. Serpico and G. Zaharijas, Astropart. Phys., 2008, 29: 380, arXiv: 0802.3245
319. M. Kuhlen, J. Diemand, and P. Madau, Astrophys. J., 2008, 686: 262, arXiv: 0805.4416
320. V. Springel, S. White, C. Frenk, J. Navarro, A. Jenkins, M. Vogelsberger, J. Wang, A. Ludlow, and A. Helmi, Nature, 2008, 456(7218): 73
321. M. R. Buckley and D. Hooper, Phys. Rev. D, 2010, 82: 063501, arXiv: 1004.1644

322. H. Zechlin, M. Fernandes, D. Elsaesser, and D. Horns, Astron. Astrophys., 2012, 538: A93, arXiv: 1111.3514
323. A. V. Belikov, D. Hooper, and M. R. Buckley, Phys. Rev. D, 2012, 86: 043504, arXiv: 1111.2613
324. M. Ackermann, et al. [Fermi-LAT Collaboration], Astrophys. J., 2012, 747: 121, arXiv: 1201.2691
325. H.-S. Zechlin and D. Horns, J. Cosmol. Astropart. Phys., 2012, 1211: 050, arXiv: 1210.3852
326. K. Belotsky, A. Kirillov, and M. Y. Khlopov, arXiv: 1212.6087, 2012
327. E. J. Baxter, S. Dodelson, S. M. Koushiappas, and L. E. Strigari, Phys. Rev. D, 2010, 82: 123511, arXiv: 1006.2399
328. S. Blanchet and J. Lavalle, J. Cosmol. Astropart. Phys., 2012, 1211: 021, arXiv: 1207.2476
329. D. Dixon, D. Hartmann, E. Kolaczyk, J. Samimi, R. Diehl, G. Kanbach, H. Mayer-Hasselwander, and A. W. Strong, New Astron., 1998, 3(7): 539, arXiv: astro-ph/9803237
330. D. Hooper and P. D. Serpico, J. Cosmol. Astropart. Phys., 2007, 0706: 013, arXiv: astro-ph/0702328
331. V. Berezinsky, V. Dokuchaev, and Y. Eroshenko, J. Cosmol. Astropart. Phys., 2007, 0707: 011, arXiv: astro-ph/0612733
332. L. Pieri, J. Lavalle, G. Bertone, and E. Branchini, Phys. Rev. D, 2011, 83: 023518, arXiv: 0908.0195
333. J. M. Siegal-Gaskins, J. Cosmol. Astropart. Phys., 2008, 0810: 040, arXiv: 0807.1328
334. M. Fornasa, L. Pieri, G. Bertone, and E. Branchini, Phys. Rev. D, 2009, 80: 023518, arXiv: 0901.2921
335. S. Ando, Phys. Rev. D, 2009, 80: 023520, arXiv: 0903.4685
336. A. Cuoco, A. Sellerholm, J. Conrad, and S. Hannestad, Mon. Not. R. Astron. Soc., 2011, 414: 2040, arXiv: 1005.0843
337. D. Malyshev, J. Bovy, and I. Cholis, Phys. Rev. D, 2011, 84: 023013, arXiv: 1007.4556
338. L. Zhang, F. Miniati, and G. Sigl, arXiv: 1008.1801, 2010
339. M. Fornasa, J. Zavala, M. A. Sanchez-Conde, J. M. Siegal-Gaskins, et al., arXiv: 1207.0502, 2012
340. A. Abdo, et al. [Fermi-LAT Collaboration], Phys. Rev. Lett., 2010, 104: 101101, arXiv: 1002.3603
341. M. Ackermann, 4th Fermi Symposium, 2012
342. A. Abdo, et al. [Fermi-LAT Collaboration], J. Cosmol. Astropart. Phys., 2010, 1004: 014, arXiv: 1002.4415
343. K. N. Abazajian, P. Agrawal, Z. Chacko, and C. Kilic, J. Cosmol. Astropart. Phys., 2010, 1011: 041, arXiv: 1002.3820
344. G. Hutsi, A. Hektor, and M. Raidal, J. Cosmol. Astropart. Phys., 2010, 1007: 008, arXiv: 1004.2036
345. C. Arina and M. H. Tytgat, J. Cosmol. Astropart. Phys., 2011, 1101: 011, arXiv: 1007.2765
346. K. N. Abazajian, S. Blanchet, and J. P. Harding, Phys. Rev. D, 2012, 85: 043509, arXiv: 1011.5090
347. J. Zavala, M. Vogelsberger, T. R. Slatyer, A. Loeb, and V. Springel, Phys. Rev. D, 2011, 83: 123513, arXiv: 1103.0776
348. Q. Yuan, B. Yue, B. Zhang, and X. Chen, J. Cosmol. Astropart. Phys., 2011, 1104: 020, arXiv: 1104.1233
349. F. Calore, V. De Romeri, and F. Donato, Phys. Rev. D, 2012, 85: 023004, arXiv: 1105.4230
350. Y.-P. Yang, L. Feng, X.-Y. Huang, X. Chen, et al., J. Cosmol. Astropart. Phys., 2011, 1112: 020, arXiv: 1112.6229
351. K. Murase and J. F. Beacom, J. Cosmol. Astropart. Phys., 2012, 1210: 043, arXiv: 1206.2595
352. S. Ando, E. Komatsu, T. Narumoto, and T. Totani, Phys. Rev. D, 2007, 75(6): 063519, arXiv: astro-ph/0612467
353. A. Cuoco, J. Brandbyge, S. Hannestad, T. Haugboelle, and G. Miele, Phys. Rev. D, 2008, 77: 123518, arXiv: 0710.4136
354. M. Taoso, S. Ando, G. Bertone, and S. Profumo, Phys. Rev. D, 2009, 79: 043521, arXiv: 0811.4493
355. J. M. Siegal-Gaskins and V. Pavlidou, Phys. Rev. Lett., 2009, 102: 241301, arXiv: 0901.3776
356. B. S. Hensley, J. M. Siegal-Gaskins, and V. Pavlidou, Astrophys. J., 2010, 723: 277, arXiv: 0912.1854
357. B. S. Hensley, V. Pavlidou, and J. M. Siegal-Gaskins, arXiv: 1210.7239, 2012
358. M. Ackermann, et al. [Fermi-LAT Collaboration], Phys. Rev. D, 2012, 85: 083007, arXiv: 1202.2856
359. L. Bergstrom and H. Snellman, Phys. Rev. D, 1988, 37(12): 3737
360. S. Rudaz, Phys. Rev. D, 1989, 39(12): 3549
361. L. Bergstrom and P. Ullio, Nucl. Phys. B, 1997, 504(1–2): 27, arXiv: hep-ph/9706232
362. Z. Bern, P. Gondolo, and M. Perelstein, Phys. Lett. B, 1997, 411(1–2): 86, arXiv: hep-ph/9706538
363. P. Ullio and L. Bergstrom, Phys. Rev. D, 1998, 57(3): 1962, arXiv: hep-ph/9707333
364. L. Bergstrom, T. Bringmann, M. Eriksson, and M. Gustafsson, Phys. Rev. Lett., 2005, 94(13): 131301, arXiv: astro-ph/0410359
365. A. Birkedal, K. T. Matchev, M. Perelstein, and A. Spray, arXiv: hep-ph/0507194, 2005
366. L. Bergstrom, T. Bringmann, M. Eriksson, and M. Gustafsson, Phys. Rev. Lett., 2005, 95(24): 241301, arXiv: hep-ph/0507229
367. T. Bringmann, L. Bergstrom, and J. Edsjo, J. High Energy Phys., 2008, 0801: 049, arXiv: 0710.3169
368. T. Bringmann, X. Huang, A. Ibarra, S. Vogl, and C. Weniger, J. Cosmol. Astropart. Phys., 2012, 1207: 054, arXiv: 1203.1312
369. C. Weniger, J. Cosmol. Astropart. Phys., 2012, 1208: 007, arXiv: 1204.2797
370. E. Tempel, A. Hektor, and M. Raidal, J. Cosmol. Astropart. Phys., 2012, 1209: 032, arXiv: 1205.1045
371. M. Su and D. P. Finkbeiner, arXiv: 1206.1616, 2012
372. A. Boyarsky, D. Malyshev, and O. Ruchayskiy, arXiv: 1205.4700, 2012
373. A. Albert, 4th Fermi Symposium, 2012
374. A. Hektor, M. Raidal, and E. Tempel, arXiv: 1207.4466, 2012

375. A. Geringer-Sameth and S. M. Koushiappas, Phys. Rev. D, 2012, 86: 021302, arXiv: 1206.0796
376. P. Nolan, et al. [Fermi-LAT Collaboration], Astrophys. J. Suppl., 2012, 199: 31, arXiv: 1108.1435
377. M. Su and D. P. Finkbeiner, arXiv: 1207.7060, 2012
378. D. Hooper and T. Linden, Phys. Rev. D, 2012, 86: 083532, arXiv: 1208.0828
379. A. Hektor, M. Raidal, and E. Tempel, arXiv: 1208.1996
380. D. Whiteson, J. Cosmol. Astropart. Phys., 2012, 1211: 008, arXiv: 1208.3677
381. A. Hektor, M. Raidal, and E. Tempel, arXiv: 1209.4548, 2012
382. D. P. Finkbeiner, M. Su, and C. Weniger, arXiv: 1209.4562, 2012
383. F. Aharonian, D. Khangulyan, and D. Malyshev, arXiv: 1207.0458, 2012
384. S. Profumo and T. Linden, J. Cosmol. Astropart. Phys., 2012, 1207: 011, arXiv: 1204.6047
385. E. Dudas, Y. Mambrini, S. Pokorski, and A. Romagnoni, J. High Energy Phys., 2012, 1210: 123, arXiv: 1205.1520
386. J. M. Cline, Phys. Rev. D, 2012, 86: 015016, arXiv: 1205.2688
387. K.-Y. Choi and O. Seto, Phys. Rev. D, 2012, 86: 043515, arXiv: 1205.3276
388. B. Kyae and J.-C. Park, arXiv: 1205.4151, 2012
389. H. M. Lee, M. Park, and W.-I. Park, Phys. Rev. D, 2012, 86: 103502, arXiv: 1205.4675
390. A. Rajaraman, T. M. Tait, and D. Whiteson, J. Cosmol. Astropart. Phys., 2012, 1209: 003, arXiv: 1205.4723
391. B. S. Acharya, G. Kane, P. Kumar, R. Lu, and B. Zheng, arXiv: 1205.5789, 2012
392. M. R. Buckley and D. Hooper, Phys. Rev. D, 2012, 86: 043524, arXiv: 1205.6811
393. X. Chu, T. Hambye, T. Scarna, and M. H. Tytgat, Phys. Rev. D, 2012, 86: 083521, arXiv: 1206.2279
394. D. Das, U. Ellwanger, and P. Mitropoulos, J. Cosmol. Astropart. Phys., 2012, 1208: 003, arXiv: 1206.2639
395. Z. Kang, T. Li, J. Li, and Y. Liu, arXiv: 1206.2863, 2012
396. N. Weiner and I. Yavin, Phys. Rev. D, 2012, 86: 075021, arXiv: 1206.2910
397. I. Oda, arXiv: 1207.1537, 2012
398. J.-C. Park and S. C. Park, arXiv: 1207.4981, 2012
399. S. Tulin, H.-B. Yu, and K. M. Zurek, arXiv: 1208.0009, 2012
400. T. Li, J. A. Maxin, D. V. Nanopoulos, and J. W. Walker, Eur. Phys. J. C, 2012, 72: 2246, arXiv: 1208.1999
401. J. M. Cline, G. D. Moore, and A. R. Frey, Phys. Rev. D, 2012, 86: 115013, arXiv: 1208.2685
402. Y. Bai and J. Shelton, J. High Energy Phys., 2012, 1212: 056, arXiv: 1208.4100
403. L. Bergstrom, Phys. Rev. D, 2012, 86: 103514, arXiv: 1208.6082
404. L. Wang and X.-F. Han, arXiv: 1209.0376, 2012
405. J. Fan and M. Reece, arXiv: 1209.1097, 2012
406. H. M. Lee, M. Park, and W.-I. Park, J. High Energy Phys., 2012, 1212: 037, arXiv: 1209.1955
407. S. Baek, P. Ko, and E. Senaha, arXiv: 1209.1685, 2012
408. B. Shakya, arXiv: 1209.2427, 2012
409. F. D'Eramo, M. McCullough, and J. Thaler, arXiv: 1210.7817, 2012
410. K. Schmidt-Hoberg, F. Staub, and M. W. Winkler, arXiv: 1211.2835, 2012
411. Y. Farzan and A. R. Akbarieh, arXiv: 1211.4685, 2012
412. G. Chalons, M. J. Dolan, and C. McCabe, arXiv: 1211.5154, 2012
413. A. Rajaraman, T. M. Tait, and A. M. Wijangco, arXiv: 1211.7061, 2012
414. Y. Bai, M. Su, and Y. Zhao, arXiv: 1212.0864, 2012
415. Y. Zhang, arXiv: 1212.2730, 2012
416. Y. Bai, V. Barger, L. L. Everett, and G. Shaughnessy, arXiv: 1212.5604, 2012
417. H. M. Lee, M. Park, and V. Sanz, arXiv: 1212.5647, 2012
418. W. Buchmuller and M. Garny, J. Cosmol. Astropart. Phys., 2012, 1208: 035, arXiv: 1206.7056
419. T. Cohen, M. Lisanti, T. R. Slatyer, and J. G. Wacker, J. High Energy Phys., 2012, 1210: 134, arXiv: 1207.0800
420. I. Cholis, M. Tavakoli, and P. Ullio, Phys. Rev. D, 2012, 86: 083525, arXiv: 1207.1468
421. L. Feng, Q. Yuan, and Y.-Z. Fan, arXiv: 1206.4758, 2012
422. R. Laha, K. C. Y. Ng, B. Dasgupta, and S. Horiuchi, arXiv: 1208.5488, 2012
423. M. Asano, T. Bringmann, G. Sigl, and M. Vollmann, arXiv: 1211.6739, 2012
424. R.-Z. Yang, Q. Yuan, L. Feng, Y.-Z. Fan, and J. Chang, Phys. Lett. B, 2012, 715: 285, arXiv: 1207.1621
425. K. Rao and D. Whiteson, arXiv: 1210.4934, 2012
426. M. Kuhlen, J. Guedes, A. Pillepich, P. Madau, and L. Mayer, arXiv: 1208.4844, 2012
427. D. Gorbunov and P. Tinyakov, arXiv: 1212.0488, 2012
428. CALET, http://calet.phys.lsu.edu/
429. Y. Li and Q. Yuan, Phys. Lett. B, 2012, 715: 35, arXiv: 1206.2241
430. Y. Becherini, et al. [HESS Collaboration], AIP Conf. Proc., 2009, 1085: 738
431. L. Bergstrom, G. Bertone, J. Conrad, C. Farnier, and C. Weniger, J. Cosmol. Astropart. Phys., 2012, 1211: 025, arXiv: 1207.6773
432. M. Actis, et al. [CTA Consortium], Exp. Astron., 2011, 32: 193, arXiv: 1008.3703
433. M. Wood, G. Blaylock, S. Bradbury, J. Buckley, et al., Astrophys. J., 2008, 678: 594, arXiv: 0801.1708
434. F. Aharonian [HESS Collaboration], Astropart. Phys., 2008, 29: 55, arXiv: 0711.2369
435. F. Aharonian, et al. [HESS Collaboration], Phys. Rev. D, 2008, 78: 072008, arXiv: 0806.2981

436. F. Aharonian [HESS Collaboration], Astropart. Phys., 2009, 34: 608, arXiv: 0809.3894
437. A. Abramowski, et al. [HESS Collaboration], Astropart. Phys., 2011, 34: 608, arXiv: 1012.5602
438. A. Abramowski, et al. [HESS Collaboration], Phys. Rev. Lett., 2011, 106: 161301, arXiv: 1103.3266
439. A. Abramowski, et al. [HESS Collaboration], Astrophys. J., 2011, 735: 12, arXiv: 1104.2548
440. E. Aliu, et al. [MAGIC Collaboration], Astrophys. J., 2009, 697: 1299, arXiv: 0810.3561
441. J. Aleksic, et al. [MAGIC Collaboration], J. Cosmol. Astropart. Phys., 2011, 1106: 035, arXiv: 1103.0477
442. E. Aliu, et al. [VERITAS Collaboration], Phys. Rev. D, 2012, 85: 062001, arXiv: 1202.2144
443. M. Doro, et al. [CTA collaboration], arXiv: 1208.5356, 2012
444. K. D. Hoffman, New J. Phys., 2009, 11: 055006, arXiv: 0812.3809
445. H. H. Chang [IceCube Collaboration], arXiv: 1209.0698, 2012
446. T. Tanaka, et al. [Super-Kamiokande Collaboration], Astrophys. J., 2011, 742: 78, arXiv: 1108.3384
447. G. Lambard [ANTARES Collaboration], arXiv: 1112.0478, 2011
448. M. G. Aartsen, et al. [IceCube Collaboration], arXiv: 1212.4097, 2012
449. R. Abbasi, et al. [IceCube Collaboration], arXiv: 1210.3557, 2012
450. F. Halzen and D. Hooper, New J. Phys., 2009, 11: 105019, arXiv: 0910.4513
451. A. E. Erkoca, M. H. Reno, and I. Sarcevic, Phys. Rev. D, 2009, 80: 043514, arXiv: 0906.4364
452. G. Wikstrom and J. Edsjo, J. Cosmol. Astropart. Phys., 2009, 0904: 009, arXiv: 0903.2986
453. M. Honda, T. Kajita, K. Kasahara, S. Midorikawa, and T. Sanuki, Phys. Rev. D, 2007, 75(4): 043006, arXiv: astro-ph/0611418
454. G. Sullivan [IceCube Collaboration], arXiv: 1210.4195, 2012
455. J. Faulkner and R. L. Gilliland, Astrophys. J., 1985, 299: 994
456. W. H. Press and D. N. Spergel, Astrophys. J., 1985, 296: 679
457. J. Silk, K. A. Olive, and M. Srednicki, Phys. Rev. Lett., 1985, 55(2): 257
458. A. Gould, Astrophys. J., 1992, 388: 348
459. A. Gould, Astrophys. J., 1987, 321: 571
460. A. Menon, R. Morris, A. Pierce, and N. Weiner, Phys. Rev. D, 2010, 82: 015011, arXiv: 0905.1847
461. S. Nussinov, L.-T. Wang, and I. Yavin, J. Cosmol. Astropart. Phys., 2009, 0908: 037, 0905.1333.
462. J. Shu, P.-F. Yin, and S.-H. Zhu, Phys. Rev. D, 2010, 81: 123519, arXiv: 1001.1076
463. M. Cirelli, N. Fornengo, T. Montaruli, I. A. Sokalski, A. Strumia, and F. Vissani, Nucl. Phys. B, 2005, 727(1–2): 99, arXiv: hep-ph/0506298
464. M. Blennow, J. Edsjo, and T. Ohlsson, J. Cosmol. Astropart. Phys., 2008, 0801: 021, arXiv: 0709.3898
465. V. Barger, W.-Y. Keung, G. Shaughnessy, and A. Tregre, Phys. Rev. D, 2007, 76: 095008, arXiv: 0708.1325
466. E. Behnke, J. Behnke, S. J. Brice, D. Broemmelsiek, J. I. Collar, P. S. Cooper, M. Crisler, C. E. Dahl, D. Fustin, J. Hall, J. H. Hinnefeld, M. Hu, I. Levine, E. Ramberg, T. Shepherd, A. Sonnenschein, and M. Szydagis, Phys. Rev. Lett., 2011, 106: 021303, arXiv: 1008.3518
467. H. Silverwood, P. Scott, M. Danninger, C. Savage, et al., arXiv: 1210.0844, 2012
468. Z. Ahmed, et al. [CDMS Collaboration and EDEL-WEISS Collaboration], Phys. Rev. D, 2011, 84: 011102, arXiv: 1105.3377
469. E. Aprile, et al. [XENON100 Collaboration], Phys. Rev. Lett., 2011, 107: 131302, arXiv: 1104.2549
470. H. Yuksel, S. Horiuchi, J. F. Beacom, and S. Ando, Phys. Rev. D, 2007, 76: 123506, arXiv: 0707.0196
471. S. Palomares-Ruiz, Phys. Lett. B, 2008, 665: 50, arXiv: 0712.1937
472. A. E. Erkoca, G. Gelmini, M. H. Reno, and I. Sarcevic, Phys. Rev. D, 2010, 81: 096007, arXiv: 1002.2220
473. P.-f. Yin, J. Liu, Q. Yuan, X.-j. Bi, and S.-h. Zhu, Phys. Rev. D, 2008, 78: 065027, arXiv: 0806.3689
474. J. Liu, P.-F. Yin, and S.-H. Zhu, Phys. Rev. D, 2009, 79: 063522, arXiv: 0812.0964
475. P. Sandick, D. Spolyar, M. R. Buckley, K. Freese, and D. Hooper, Phys. Rev. D, 2010, 81: 083506, arXiv: 0912.0513
476. B. Dasgupta and R. Laha, Phys. Rev. D, 2012, 86: 093001, arXiv: 1206.1322
477. K. Murase and J. F. Beacom, arXiv: 1209.0225, 2012
478. L. Bergstrom, P. Ullio, and J. H. Buckley, Astropart. Phys., 1998, 9(2): 137, arXiv: astro-ph/9712318
479. R. Abbasi, et al. [IceCube Collaboration], Astropart. Phys., 2012, 35: 615, arXiv: 1109.6096
480. R. Abbasi, et al. [IceCube Collaboration], Phys. Rev. D, 2011, 84: 022004, arXiv: 1101.3349
481. C. Rott [IceCube Collaboration], in: the IDM 2012 Conference, 23–27 July, Chicago, 2012